



**HAL**  
open science

## Comparison of methane yield of a novel strain of *Methanothermobacter marburgensis* in pure and mixed adapted culture derived from a methanation bubble column bioreactor

Corinne Biderre-Petit, Mbarki Mariem, Damien Courtine, Benarab Yanis, Christophe Vial, Pierre Fontanille, Pascal Dubessay, Misagh Keramati, Isabelle Jouan-Dufournel, Arthur Monjot, et al.

### ► To cite this version:

Corinne Biderre-Petit, Mbarki Mariem, Damien Courtine, Benarab Yanis, Christophe Vial, et al.. Comparison of methane yield of a novel strain of *Methanothermobacter marburgensis* in pure and mixed adapted culture derived from a methanation bubble column bioreactor. *Bioresource Technology*, inPress, 406, pp.131021. 10.1016/j.biortech.2024.131021 . hal-04621855v2

**HAL Id: hal-04621855**

**<https://hal.science/hal-04621855v2>**

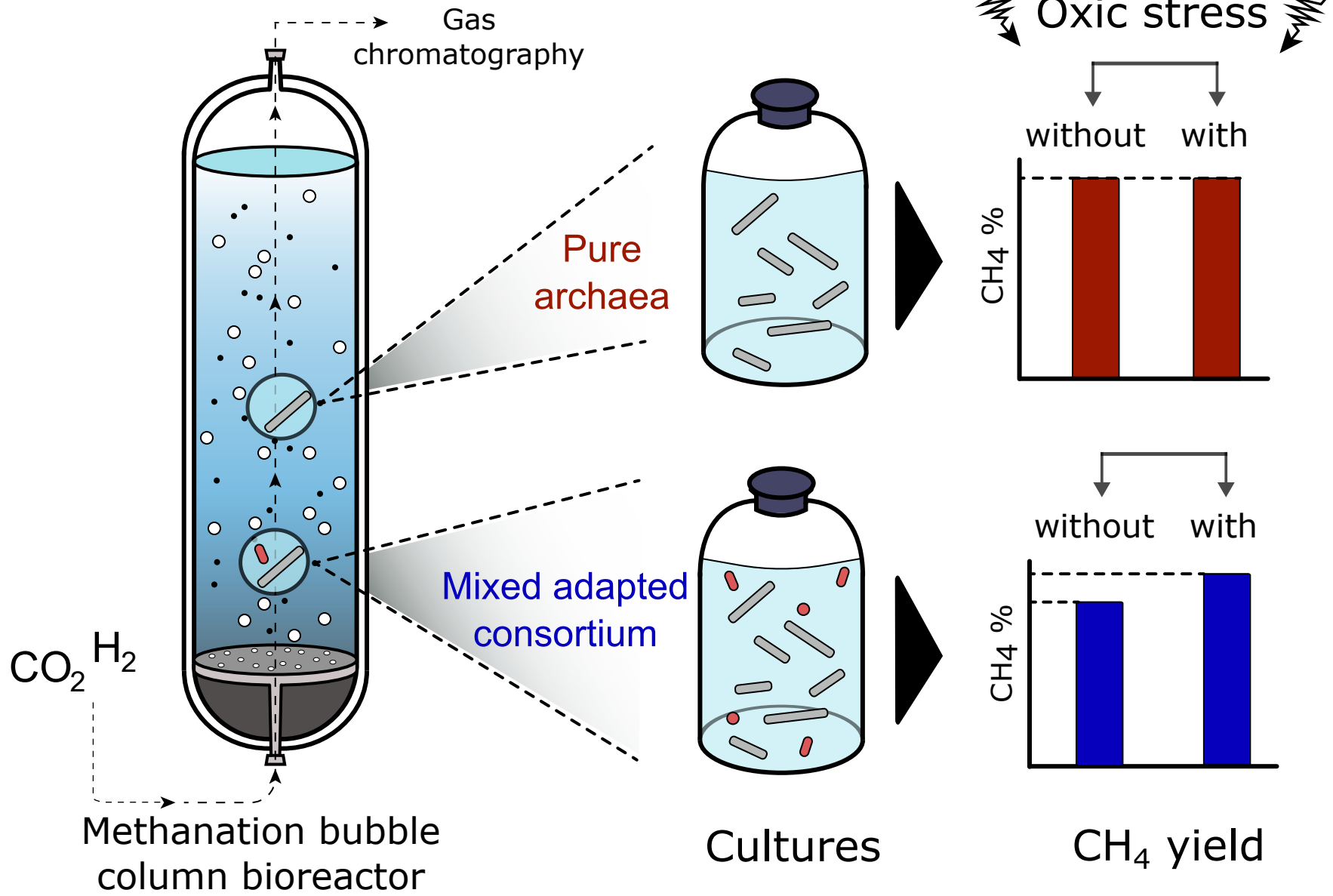
Submitted on 24 Jun 2024

**HAL** is a multi-disciplinary open access archive for the deposit and dissemination of scientific research documents, whether they are published or not. The documents may come from teaching and research institutions in France or abroad, or from public or private research centers.

L'archive ouverte pluridisciplinaire **HAL**, est destinée au dépôt et à la diffusion de documents scientifiques de niveau recherche, publiés ou non, émanant des établissements d'enseignement et de recherche français ou étrangers, des laboratoires publics ou privés.



Distributed under a Creative Commons Attribution - NonCommercial 4.0 International License



## Highlights

1. Archaeal cell enumeration using flow cytometry
2. MBA03 association with *Methanothermobacter* as an indicator of process stability
3. O<sub>2</sub> exposure impacts CH<sub>4</sub> yield of the consortium but not that of pure strains
4. Two *Methanothermobacter marburgensis* strains with different growth behaviour

## Title

Comparison of methane yield of a novel strain of *Methanothermobacter marburgensis* in pure and mixed adapted culture derived from a methanation bubble column bioreactor

## Authors

Biderre-Petit Corinne<sup>1\*</sup>, Mbarki Mariem<sup>1</sup>, Courtine Damien<sup>1</sup>, Benarab Yanis<sup>1</sup>, Vial Christophe<sup>2</sup>, Fontanille Pierre<sup>2</sup>, Dubessay Pascal<sup>2</sup>, Keramati Misagh<sup>2</sup>, Jouan-Dufournel Isabelle<sup>1</sup>, Monjot Arthur<sup>1</sup>, Guez Jean Sébastien<sup>2</sup> and Fadhlaoui Khaled<sup>1,3\*</sup>

<sup>1</sup>Université Clermont Auvergne, CNRS, Laboratoire Microorganismes : Génome et Environnement, F-63000, Clermont-Ferrand, France.

<sup>2</sup>Université Clermont Auvergne, Clermont Auvergne INP, CNRS, Institut Pascal, 63000 Clermont-Ferrand, France.

<sup>3</sup>Université Clermont Auvergne, UMR 454 MEDIS UCA-INRAE, F-63000 Clermont-Ferrand, France

\*For correspondence: Corinne Biderre-Petit, 1 Impasse Amélie Murat - Bat BioA 63178 Aubière (France). E-mail: [corinne.petit@uca.fr](mailto:corinne.petit@uca.fr), Tel: +33(0)473405139; Fax+33 (0)473407670; Khaled Fadhlaoui, 1 Impasse Amélie Murat - Bat BioA 63178 Aubière (France). E-mail: [khaled.fadhlaoui@uca.fr](mailto:khaled.fadhlaoui@uca.fr), Tel: +33(0)473177959; Fax+33 (0)473407670.

E-mails: C Petit: [corinne.petit@uca.fr](mailto:corinne.petit@uca.fr); M Mbarki: [mmbarki342@gmail.com](mailto:mmbarki342@gmail.com); D Courtine: [Damien.courtine@uca.fr](mailto:Damien.courtine@uca.fr); Y Benarab: [benarabyanis0@gmail.com](mailto:benarabyanis0@gmail.com); C Vial: [christophe.vial@uca.fr](mailto:christophe.vial@uca.fr); P Fontanille: [pierre.fontanille@uca.fr](mailto:pierre.fontanille@uca.fr), P Dubessay: [pascal.dubessay@uca.fr](mailto:pascal.dubessay@uca.fr); M Keramati: [Misagh.KERAMATI@uca.fr](mailto:Misagh.KERAMATI@uca.fr); I Jouan-Dufournel: [Isabelle.JOUAN@uca.fr](mailto:Isabelle.JOUAN@uca.fr); A Monjot: [arthur.monjot.pro@gmail.com](mailto:arthur.monjot.pro@gmail.com); JS Guez: [j-sebastien.guez@uca.fr](mailto:j-sebastien.guez@uca.fr); K Fadhlaoui: [Khaled.fadhlaoui@uca.fr](mailto:Khaled.fadhlaoui@uca.fr)

## **Acknowledgements**

The authors would like to acknowledge Hermine Billard and Jonathan Colombet, Plateforme SYSTEM – UCA PARTNER (Clermont-Ferrand, France), for their technical support and expertise. We also thank Pr. Cécile Lepère and Dr. Bernard Ollivier for their thorough reviewing of the manuscript.

## **Funding sources**

This work was sponsored by the French government research program through ANR BIOMINTENS [grant number ANR-20-CE05-0031, 2021].

## 1 **Title**

2 Comparison of methane yield of a novel strain of *Methanothermobacter marburgensis*  
3 in pure and mixed adapted culture derived from a methanation bubble column  
4 bioreactor

5

## 6 **Abstract**

7 The ongoing discussion regarding the use of mixed or pure cultures of  
8 hydrogenotrophic methanogenic archaea in Power-to-Methane (P2M) bioprocess  
9 applications persists, with each option presenting its own advantages and disadvantages.  
10 To address this issue, a comparison of methane (CH<sub>4</sub>) yield between a novel  
11 methanogenic archaeon belonging to the species *Methanothermobacter marburgensis*  
12 (strain Clermont) isolated from a biological methanation column, and the community  
13 from which it originated, was conducted. This comparison included the type strain *M.*  
14 *marburgensis* str. Marburg. The evaluation also examined how exposure to oxygen (O<sub>2</sub>)  
15 for up to 240 minutes impacted the CH<sub>4</sub> yield across these cultures. While both  
16 *Methanothermobacter* strains exhibit comparable CH<sub>4</sub> yield, slightly higher than that of  
17 the mixed adapted culture under non-O<sub>2</sub>-exposed conditions, strain Clermont does not  
18 display the lag time observed for strain Marburg.

19

## 20 **Keywords**

21 *Methanothermobacter marburgensis*, mixed hydrogenotrophic methanogenic culture,  
22 oxygen exposure, multi-omics approaches.

23

## 24 **1. Introduction**

25 To limit the rise of global surface temperature to less than 2°C while meeting the  
26 increasing energy demand, a significant global energy transition is urgently needed.  
27 However, shifting away from polluting fossil fuels to low-carbon solutions requires  
28 technological innovation, particularly in renewable energy. Despite substantial progress  
29 in wind, solar, and geothermal energies, challenges such as intermittency, variability,  
30 geographical limitations, and storage persist (Tong et al., 2021). Power-To-Gas (P2G)  
31 concept has emerged as a promising solution allowing the storage of surplus of  
32 renewable energy recovered from the electricity sector in the form of gas (*i.e.*  
33 dihydrogen (H<sub>2</sub>) called P2H and CH<sub>4</sub> called P2M) (Glenk and Reichelstein, 2022).  
34 Currently, P2M offers advantages over P2H. It allows converting electricity into  
35 chemical energy and uses existing infrastructure. Considering storability, it has a higher  
36 energy density (10 kWh/Nm<sup>3</sup> for CH<sub>4</sub> versus 3 kWh/Nm<sup>3</sup> for H<sub>2</sub>) and is suitable for  
37 long term and large-scale storage (Blanco et al., 2018). P2M systems combine H<sub>2</sub>  
38 oxidation and carbon dioxide (CO<sub>2</sub>) reduction to produce CH<sub>4</sub> using either  
39 physicochemical or biological catalysts (biomethanation). Comparatively,  
40 biomethanation processes require lower temperatures and pressures than  
41 physicochemical methanation processes and exhibit increased resistance to chemical  
42 contaminants including hydrogen sulfide (H<sub>2</sub>S), organic acids, or ammonia (Burkhardt  
43 et al., 2015).  
44 Hydrogenotrophic methanogenic archaea (HMs), which can use H<sub>2</sub> as a reducing agent  
45 for the conversion of CO<sub>2</sub> into CH<sub>4</sub>, are key biocatalysts for biomethane (Bellini et al.,  
46 2022). They require as much H<sub>2</sub> as the system can provide for CO<sub>2</sub> reduction.  
47 Therefore, the competition and sustainable equilibrium between H<sub>2</sub> producers (*e.g.*  
48 acetogens) and consumers (*e.g.* HMs) usually result in a very low dissolved H<sub>2</sub> partial

49 pressure ( $p(\text{H}_2)$ ) to maintain a balanced operation of the entire microbiological  
50 community. However, numerous abiotic and biotic factors can affect this equilibrium.  
51 From a thermodynamical perspective, external  $\text{H}_2$  provision strongly favours  
52 hydrogenotrophic methanogenesis. But a sudden increment of  $p(\text{H}_2)$  can enable the  
53 homoacetogenic pathway to outcompete the hydrogenotrophic methanogenesis (Treu et  
54 al., 2018; Tsapekos et al., 2022). In addition, temperature, pH,  $\text{H}_2/\text{CO}_2$  ratio,  $\text{H}_2$  supply,  
55 etc, are all abiotic factors that can influence  $\text{CH}_4$  content and microbial community  
56 during *in-situ* biological biogas upgrading (Rachbauer et al., 2017; Wahid et al., 2019).  
57 Among HMs, the main actors in biomethanation processes comprise members of the  
58 genera *Methanoculleus*, *Methanothermobacter*, *Methanobacterium*, or *Methanosarcina*.  
59 The relative abundance of these genera in biogas upgrading reactors varies based on  
60 factors such as temperature, pH, carbon monoxide (CO), etc (Thema et al., 2021; Xu et  
61 al., 2020). In thermophilic conditions, *Methanothermobacter* was shown to be  
62 predominant in the mixed cultures due to its favorable growth at higher temperatures  
63 (Kaster et al., 2011; Szuhaj et al., 2021). Within this genus, *Methanothermobacter*  
64 *thermautotrophicus* and *Methanothermobacter marburgensis*, largely used as model  
65 organisms, have already been implemented as biocatalysts in large-scale industrial  
66 processes because they are robust, and reach high cell densities, and  $\text{CH}_4$  production  
67 rate (Seifert et al., 2014; Pfeifer et al., 2021; Thema et al., 2021, Kaul et al., 2022).  
68 Two main approaches can be employed for biomethanation, *i.e.* using pure cultures or  
69 enriched mixed cultures, each with its own advantages and drawbacks (Rachbauer et al.,  
70 2017; Rafrafi et al., 2021; Rittmann et al., 2018). Indeed, using single self-replicating  
71 catalysts would prevent oxidation of  $\text{H}_2$  by other hydrogenotrophic microorganisms,  
72 thereby avoiding a loss of efficiency in biogas upgrading. It would also allow for better



73 system variability and behaviour prediction (Martin et al., 2013). On the other hand,  
74 using consortia would be more efficient, leading to larger CH<sub>4</sub> yields (Bellini et al,  
75 2022, Paniagua et al., 2022). Other advantages of employing consortia include greater  
76 robustness and short recovery time upon starvation/excess input gas rate and  
77 oxygenation. However, managing mixed cultures often requires increased control and a  
78 thorough understanding of how microbial composition impacts the system (Paniagua et  
79 al., 2022). Therefore, despite the growing number of studies in this field, the question of  
80 whether pure or mixed cultures are more suitable for biomethanation processes remains  
81 unresolved. To address this question, a comparison of the performance of both HM pure  
82 cultures and reactor microbiomes from which HMs have been isolated appears essential.  
83 This study aims to evaluate the methanation efficiency of a new HM affiliated to the *M.*  
84 *marburgensis* species (strain Clermont) isolated from a bubble column reactor. Its  
85 methanogenic performance was compared not only with its native consortium but also  
86 with the type strain, *i.e.* *M. marburgensis* strain Marburg (hereinafter referred to as  
87 strain Marburg). This comparison was extended under oxidative stress, a common  
88 occurrence in biomethanation processes.

89

## 90 **2. Material and Methods**

### 91 **2.1. Laboratory-scale methanation reactor**

92 The mixed adapted culture used in this study was collected from a 3.5 L bubble column  
93 reactor, six weeks after its inoculation with 300 mL of digestate from a thermophilic  
94 industrial-scale biogas plant treating livestock effluent and agri-food industry wastes  
95 that operates between 52 and 54°C (Methelec, Ennezat, France). Briefly, the reactor  
96 contained 2.7 L of basal anaerobic (BA) culture medium prepared as previously  
97 reported (Bu et al., 2018) and reduced by introducing 0.4 g/L of sodium sulfide

98 nanohydrate ( $\text{Na}_2\text{S}\cdot 9\text{H}_2\text{O}$ ). The  $\text{H}_2/\text{CO}_2$  gas mixture was set at a ratio of 4:1 (v/v) with a  
99 mass flowmeter (SLA5800, Brooks Instrument, Hatfield, USA). Flow rates ranged from  
100 0.29 to 0.44  $\text{NL}\cdot\text{min}^{-1}$ . The temperature was set to  $55^\circ\text{C}$  using a thermostatic bath (Eco  
101 RE1225 silver, Lauda, Königshofen, Germany).

102 Volatile fatty acids (VFAs) in the six-week mixed adapted culture were determined  
103 using a liquid chromatograph (1260 HPLC, Agilent, Santa Clara, USA). The HPLC  
104 apparatus was equipped with two columns (Rezex ROA 300 x 7.8 nm, Phenomenex,  
105 Torrance, USA) mounted in serial in an oven ( $50^\circ\text{C}$ ) and coupled with a refractive index  
106 detector. The mobile phase was a 2 mM sulfuric acid in ultra-pure water pumped at 0.7  
107  $\text{mL}\cdot\text{min}^{-1}$  and 70 bars. For the analysis, 2 mL of sample were mixed with 125  $\mu\text{L}$  of  
108  $\text{Ba}(\text{OH})_2\cdot 8\text{H}_2\text{O}$  (0.3 M) and 125  $\mu\text{L}$  of  $\text{ZnSO}_4\cdot 7\text{H}_2\text{O}$  (5% w/v) before a 5 min  
109 centrifugation at 10000 g. Samples were filtered through 0.2  $\mu\text{m}$  nylon filters before  
110 being injected in the HPLC apparatus.

111 Measurements of archaeal and bacterial abundance (quantitative real-time PCR),  
112 performed on the six-week sample mixed adapted culture, revealed a dominance of  
113 archaea over bacteria with an archaea/bacteria ratio of five ( $1.0\ 10^9$  archaeal cells/mL  
114 versus  $2.2\ 10^8$  bacterial cells/mL).

## 115 **2.2. Microbial community analysis of the mixed adapted culture**

116 Two mL of the six-week mixed adapted culture were centrifuged at 10000 g at room  
117 temperature (RT) for 10 min and total genomic DNA (gDNA) was extracted from the  
118 pellet using a Nucleo Spin Soil kit in accordance with manufacturer's instructions  
119 (Machery Nagel, Düren, Germany). Then, gDNA was quantified using a  
120 spectrophotometer (NanoDrop 1000, Thermo Fisher Scientific, USA). Subsequently,  
121 the V3-V4 hypervariable region of the bacterial 16S ribosomal RNA (rRNA) genes was

122 amplified using the primer set F343 (5'-  
123 CTTTCCCTACACGACGCTCTTCCGATCTACGGRAGGCAGCAG-3') - R784 (5'-  
124 GGAGTTCAGACGTGTGCTCTTCCGATCTTACCAGGGTATCTAATCCT-3')  
125 (Carmona-Martinez et al., 2015) while the V4-V5 region of the archaeal 16S rRNA  
126 genes was amplified with the primer set F504-519 (5'-  
127 CTTTCCCTACACGACGCTCTTCCGATCTCAGCMGCCGCGGKAA-3') and R910-  
128 928 (5'-GGAGTTCAGACGTGTGCTCTTCCGATCTCCCGCCWATTCCTTTAAGT-  
129 3') (Braga Nan et al., 2020), primers containing adapters and barcodes for Miseq  
130 sequencing. PCR reactions contained Taq<sup>TM</sup> TaKaRa Premix, 1 µM of each primer, 200  
131 µM of each deoxynucleoside triphosphate (dNTP), 0.625 U TaKaRa Taq polymerase  
132 (TakaRa Inc., France), nuclease free-H<sub>2</sub>O and 50 to 100 ng gDNA template in a total  
133 volume of 50 µL. For both bacteria and archaea, after a denaturation step of 1 min at  
134 98°C, PCR steps at 98°C for 1 min, 59°C for 40 s, and 72°C for 1 min were repeated 35  
135 times, followed by an elongation step at 72°C for 10 min in a Mastercycler® thermal  
136 cycler (Eppendorf, Hamburg, Germany). Amplicon size was checked by Agilent High  
137 Sensitivity DNA Kit on 2100 Bioanalyzer (Agilent Technologies, Santa Clara, CA,  
138 USA). Amplicon libraries were prepared and sequenced by the GenoToul platform  
139 (Toulouse, France) with an Illumina MiSeq sequencer to generate 2 x 300 bp paired-end  
140 reads. Bacterial and archaeal reads were separately processed using a homemade  
141 bioinformatics pipeline. Briefly, paired reads were merged using the VSEARCH  
142 v2.18.0 (Rognes et al., 2016) and then trimmed and filtered with Cutadapt (Martin,  
143 2011) to minimize the effects of random sequencing errors as follows: (i) only merged  
144 reads with a length 200-500 bp were kept, (ii) paired reads with sequencing errors in  
145 primers were discarded and (iii) primer sequences and nucleotides with Phred quality

146 scores upper than 30 were trimmed. Deletion of chimeric sequences and clusterization  
147 were carried out using VSEARCH (Rognes et al., 2016) and operational taxonomic  
148 units (OTUs) that accounted for <0.005% of the total set of sequences were discarded  
149 (Bokulich et al., 2013). The taxonomic assignment was performed against the SILVA  
150 v138.1 SSU NR99 database using the global alignment script in VSEARCH (Pruesse et  
151 al, 2007; Rognes et al., 2016).

### 152 **2.3. Hydrogenotrophic methanogenic archaea isolation and analytical procedures**

153 A serum vial (Dutscher, Bernolsheim, France) containing 50 ml of BA medium (110  
154 mL in capacity) was inoculated with an aliquot of the six-week mixed adapted culture  
155 (10% v/v). After BA medium autoclaving, and prior to its inoculation, dinitrogen (N<sub>2</sub>)  
156 filling the head space was replaced by H<sub>2</sub>/CO<sub>2</sub> (4:1, v/v) gas mixture from a gas  
157 cylinder (Westfalen, France) at 2 bars. Liquid cultivation was conducted at 55°C in the  
158 dark, without agitation.

159 HM isolation was performed *via* successive dilution to extinction series in Hungate  
160 tubes (16.5 mL capacity) containing 5 mL of either liquid or solid BA medium (2% agar  
161 w/v; roll-tube technique (Hungate, 1969)). Headspace composition was determined by  
162 gas chromatography (3000A MicroGC, Agilent Technologies, Santa Clara, CA, USA)  
163 equipped with two capillary columns (one MS-5A column associated with a backflush  
164 injector and one PorapLOT Q column associated with a standard injector) and Soprane  
165 software v3.5.2 for the analysis. The microGC used argon as gas carrier and the  
166 temperature of the columns and injectors were at 50 and 60°C, respectively.

167 The purity of HMs was checked by microscopic observations (Leica DM IRB inverted  
168 microscope equipped with a Hamamatsu C13440 camera and Zen Blue v3.1 software)  
169 and by adding yeast extract (2 g/L) and glucose (20 mM final concentration) to the BA

170 medium to confirm the absence of fermentative bacteria. Subsequently, HM taxonomic  
171 identification was performed by 16S rRNA gene sequence amplification using the  
172 universal primer set Arch21F-1492R (Nakagawa et al., 2006) followed by sequencing  
173 (Eurofins Genomics, Cologne, Germany). For the ultrastructural characterization, the  
174 archaeal cells in 1% (v/v) formaldehyde fixed samples were collected by centrifugation  
175 at 20000 g for 20 min at 14°C directly onto 400-mesh electron microscopy copper grids  
176 covered with carbon-coated Formvar film (AO3X, Pelanne Instruments, Toulouse,  
177 France). Particles were over contrasted with 2% uranyl salts and rinsed three times in  
178 distilled deionized water before being dried at RT. Subsequently, the characterization  
179 was performed with a transmission electron microscope using a JEOL 2100  
180 (Akishikma, Tokyo, Japan; Plateforme CYSTEM, UCA Partner, Clermont-Ferrand,  
181 France). The microscope was operated at 80 kV, and the images were recorded with an  
182 Gatan CMOS RIO 9 camera (Gatan Ametek, Pleasanton, USA) at 3072 x 3072 pixels.  
183 Since all HMs belonged to the same strain, one representative, called  
184 *Methanothermobacter marburgensis* strain Clermont (hereafter referred to as strain  
185 Clermont), was deposited in the Deutsche Sammlung von Mikroorganismen und  
186 Zellkulturen (DSMZ) culture collection (accession number DSM 34405).

#### 187 **2.4. Cultivation procedures**

188 The hydrogenotrophic and methanogenic activities of strain Clermont, the mixed  
189 adapted culture, and *M. marburgensis* strain Marburg obtained from DSMZ (DSM  
190 2133), which is the closest relative of strain Clermont (99.5% 16S rRNA gene identity),  
191 were investigated under reduced conditions. Cultures were conducted in serum vials  
192 containing 50 mL of BA medium as described above (Paragraph 2.3). All inoculations  
193 were performed with the same number of archaeal cells, *i.e.*  $5.7 \times 10^5$  cells. Briefly, an

194 aliquot of 1 mL of pure or mixed cultures at the end of the exponential growth phase  
195 was diluted to 1:10 and directly used for flow cytometry analysis (BD LSR Fortessa X-  
196 20; BD Biosciences, CA, USA). Two lasers (Violet, 405 nm, 50 mW and Blue, 488 nm,  
197 60 mW) were used for F420 cofactor excitation (autofluorescence of archaeal cells) and  
198 morphological characterization, respectively. The threshold was set at 200 on the F420  
199 cofactor parameter. Data were acquired during 60 sec at a constant flow rate of 29.85  
200  $\mu\text{L}/\text{min}$  and processed using FACSDivA 9 software (BD Biosciences).

201 Cultures subjected to oxidative stress were inoculated and grown in medium devoid of  
202 chemical reducing agents, namely  $\text{Na}_2\text{S}\cdot 9\text{H}_2\text{O}$  and resazurin, generally used to reinforce  
203 anaerobiosis and detect any potential oxidation, to prevent  $\text{O}_2$  reduction during the  
204 exposure. Indeed, their presence would have reduced the effective amount of  $\text{O}_2$  during  
205 oxic stress. Anaerobiosis prior to oxic stress was confirmed by microGC. After reaching  
206 the end of the exponential growth phase in anaerobic conditions, the cultures were  
207 transferred to sterile beakers in a laminar flow hood and placed under high stirring  
208 speed to be exposed to atmospheric levels of  $\text{O}_2$  (21%) for durations of 0, 10, 30, 60, 90,  
209 120, and 240 min. The quantity of dissolved  $\text{O}_2$  measured in the medium was  $10 \text{ mg/L} \pm$   
210  $0.32 \text{ mg/L}$  from 1 min up to 240 min of exposure (portable oximeter, Laqua 200 series,  
211 Horiba Scientific, Japan). Subsequently, fresh BA medium containing a reducing agent  
212 was inoculated as above. The absence of  $\text{O}_2$  was checked by gas chromatography before  
213 incubation.

214 All experiments were conducted in biological triplicates. During growth, gas  
215 composition in the headspace was monitored daily by gas chromatography. Statistical  
216 analysis of  $\text{CH}_4$  yield during growth was conducted using the Student t-test, one-way or  
217 two-way ANOVA (culture  $\times$  incubation days) followed by Tukey's test under normality

218 and homoscedasticity assumption. The level of significance was set at  $\alpha=0.05$ . All  
219 statistical analyses were performed using the R Stats package v4.2.2.

## 220 **2.5. DNA extraction for whole genome sequencing of the *M. marburgensis* strain**

### 221 **Clermont**

222 A culture of strain Clermont (50 mL) in exponential growth was concentrated by  
223 centrifugation for 15 min at 10000 g at RT. gDNA was extracted from the pellet using a  
224 standard phenol–chloroform method (Biderre-Petit et al, 2024) before quantification on  
225 a Qubit Fluorometer (ThermoFisher Scientific, USA) by using Qubit<sup>TM</sup> dsDNA HS  
226 assay kit in accordance with manufacturer's instructions. Subsequently, 300 ng of  
227 gDNA were sequenced using Illumina HiSeq technology (2 × 150 bp; Eurofins  
228 Genomics, Constance, Germany). Raw paired-end reads were quality-filtered with fastp  
229 v0.23.4 (Chen et al., 2018). *De novo* assembly of whole genome sequencing data was  
230 performed using Unicycler v0.5.0 (Wick et al., 2017) with default settings. In the  
231 following step, the short contigs with viral/transposable elements (BLASTX search  
232 against non-redundant database) and fragmented rRNA operons (barrnap v0.9 and  
233 parameter "--kingdom arc", <https://github.com/tseemann/barrnap>) were filtered out.

## 234 **2.6. Phylogenomic tree construction**

235 Representative genomes of *Methanothermobacterium*, *Methanonatronarchaeia*,  
236 *Archaeoglobi*, *Methanobacteria*, *Methanococci*, *Methanomicrobia*, *Methanopyri*,  
237 *Thermococci*, and *Halobacterium* were downloaded from the National Center for  
238 Biotechnology Information (NCBI) RefSeq. Subsequently, a genome-based  
239 phylogenetic tree was generated with the program GToTree v1.8.2 as reported in  
240 Biderre-Petit et al. (2024), using an archaea-specific gene set composed of 73 markers.  
241 Individual gene alignments were concatenated to construct a species tree using IQ-

242 TREE v2.2.3 with the evolution model LG+F+I+R10 and parameters "-B 2000 --alrt  
243 2000 --bnni" (Minh et al., 2020). *Halobacterium* was used as an outgroup.

## 244 **2.7. Pan-genomic analysis and other genome characterizations**

245 Pan-genomic analysis of the Marburg clade (*i.e.* including the strains Marburg,  
246 Clermont and their closest relatives-strain KEPCO-1 (assembly accession  
247 GCA\_008033705.1), strain K4 (GCA\_022014235.1), strain THM2  
248 (GCA\_009917665.1), bin GMQ\_75\_MeOH\_H2\_bin\_21 (GCA\_030055425.1) and bin  
249 JZ-3\_D\_bin\_25 (GCA\_030055435.1); seven genomes in total) was carried out using the  
250 "pan-genomics workflow of anvi'o v7.1 (Delmont and Eren, 2018). The average  
251 nucleotide identity (ANI) was also calculated through anvi'o and to complete the  
252 results, *in silico* DNA-DNA hybridization (*isDDH*) was computed using Genome-to-  
253 Genome Distance Calculator v2.1 with formula 2 as previously recommended (Meier-  
254 Kolthoff et al., 2013). Genome synteny was visualized by NGenomeSyn v1.41 (He et  
255 al., 2023).

256

## 257 **3. Results and discussion**

### 258 **3.1. Overview of microbial community diversity in a bubble column reactor**

259 Metabarcoding procedure was used to separately address the archaeal and bacterial  
260 diversity present in the six-week adapted culture. Although less abundant than archaea,  
261 bacteria showed much higher diversity, with 833 OTUs (19403 reads in total) versus 42  
262 OTUs (28482 reads), respectively, which is consistent with what is generally described  
263 for mixed cultures (Xu et al., 2020). For the archaea, the four most abundant OTUs  
264 (>1% relative abundance in the sample) covered 96.1% of the community (See  
265 supplementary material). *Methanothermobacter* genus represented 98.5% of the



266 archaeal community in terms of reads, followed by *Methanobacterium* (1.2%),  
267 *Methanomassiliicoccus* (0.09%) and *Methanoculleus* (0.01%) (Fig. 1A). This finding  
268 closely aligns with previous research, which has shown that *Methanothermobacter* is  
269 the dominant genus in the hydrogenotrophic methanogenic consortium of *ex-situ*  
270 methanation systems at 55°C (Xu et al., 2020). Within this genus, 98.9% of the reads  
271 are affiliated to the *M. marburgensis* species (>97% 16S rRNA gene sequence identity).  
272 Regarding bacteria, the most represented phyla in terms of reads were *Bacillota* (ex  
273 *Firmicutes*, 91.8% of total bacterial reads) followed by *Pseudomonadota* (ex  
274 *Proteobacteria*, 6.8%) (Fig. 1B), in agreement with previous studies (Bassani et al.,  
275 2015; Campanaro et al., 2020). The 11 most abundant OTUs (>1% relative abundance  
276 in the sample) covered 48.7% of the bacterial community (See supplementary material)  
277 and mostly affiliated with the genus *Haloplasma* (35.2% of all bacterial reads) and the  
278 class *Limnochordia* (33.2%) in *Bacillota*.  
279 The most abundant taxon, *i.e.* *Haloplasma*, is currently represented by only one  
280 representative, a halophilic bacterium isolated from a deep-sea brine lake, named *H.*  
281 *contractile*. The growth limit of this bacterium was determined at 44°C (Antunes et al.,  
282 2008), which is not in accordance with the temperature used in this study, *i.e.* 55°C.  
283 However, although SILVA classifies this predominant taxon in the genus *Haloplasma*,  
284 the sequence used as reference and which shows 99% identity with OTUs affiliated to  
285 *Haloplasma* (accession number FN436037, see supplementary material), displays only  
286 up to 89% sequence similarity with *Haloplasma* using BLAST N against the nucleotide  
287 database in NCBI. This may be due to the low number of sequences representative of  
288 the genus *Haloplasma* and also more generally of the family and order. Indeed, the  
289 order Haloplasmales currently includes a single family -Haloplasmataceae- which

290 includes a single genus and species: *H. contractile*. This most likely not only leads to an  
291 inaccurate affiliation at the genus level, but also potentially at the family level.  
292 Consequently, the representatives that will be discovered for this group of  
293 Haloplasmodiales will most certainly allow significant changes to the current description  
294 made for the single type species.

295 The second most abundant taxon, the *Limnochordia* class, is frequently observed in full-  
296 size and laboratory-scale thermophilic biogas reactors (Campanaro et al., 2020). The  
297 main representative in this class was MBA03 (14.6% of all bacterial reads).  
298 Laguillaumie et al. (2022) suggested that MBA03, referenced as a carbohydrate  
299 fermentative taxon, would grow on lysis products and prevent side products, such as  
300 VFAs, from accumulating in the reactor. The low amount of VFAs measured in the  
301 reactor could therefore be explained, at least in part, by the MBA03 abundance. This  
302 low quantity also indicates that hydrogenotrophic methanogenesis has not shifted  
303 towards homoacetogenesis. Moreover, MBA03 association with *Methanobacterium* was  
304 described as an indicator of process stability (Laguillaumie et al., 2022). Its association  
305 with *Methanothermobacter* could therefore still be such an indicator.

306 In addition to MBA03, two other bacteria known to be syntrophic acetate oxidizing, *i.e.*  
307 *Tepidiphilus* (*Pseudomonadota*) and norank order D8A-2 (*Bacillota*), showed  
308 significant relative abundance, with 2.9% and 3.6% of all bacterial reads, respectively.  
309 These results are in line with previous studies, which showed that these taxa were  
310 abundant in thermophilic samples and worked synergistically with HMs, providing the  
311 substrates they need towards biogas production (Tang et al., 2008; Xu et al., 2020). An  
312 anaerobic digestion system seeded from manure samples (which is comparable to what  
313 was used for the bioreactor, *i.e.* a biogas plant treating livestock effluent) and running at

314 55°C (Sun et al., 2015), was shown to be populated with similar microbial taxa. This  
315 supports the view that temperature, but also inoculum, are crucial variables in  
316 determining the structure of microbial consortia in hydrogenotrophic methanogenic  
317 mixed cultures (Xu et al., 2020).

### 318 **3.2. Isolation and genome sequencing of *M. marburgensis* strain Clermont**

319 The strain isolated from the bioreactor belonged to the genus *Methanothermobacter* and  
320 showed >99.5% identity with strain Marburg 16S rRNA gene sequence (accession  
321 number NR\_102881.1). It was named *M. marburgensis* strain Clermont and deposited  
322 in the DSMZ collection (DSM 34405). This strain was rod-shaped (~5 µm long and 0.6  
323 µm wide) and non-motile (See supplementary material).

324 The draft genome of strain Clermont (~330-fold coverage), featuring six contigs (from  
325 ~21.9 to 776.9 kb), had a total length of ~1.72 Mb, a N50 contig length of 593 kb, and  
326 a G+C content of 48.7%. The number of coding DNA sequences was 1805 with two  
327 16S-23S rRNA gene clusters, three 5S rRNA genes and 37 transfer RNA (tRNA) genes.  
328 No extra-chromosomal genetic elements were detected. Genome fragmentation was  
329 mainly due to the high conservation degree between rRNA operons and transposase  
330 sequences that hamper the assembly tool to resolve these loci. Phylogenomic analysis  
331 confirmed the close relationship of strain Clermont with strain Marburg but also with  
332 three other *Methanothermobacter* strains (*i.e.* KEPCO-1, THM\_2, and K4) and two bins  
333 (*i.e.* GMQ\_75\_MeOH\_H2\_bin\_21 and JZ-3\_D\_bin\_25). They all formed a clade  
334 (hereinafter referred to as Marburg clade) within the genus *Methanothermobacter* (Fig.  
335 2A). Their genomes revealed a high degree of synteny (Fig. 2B). Based on ANI and  
336 *is*DDH values, strains Clermont, Marburg, KEPCO\_1 and THM\_2 formed a single  
337 species (ANI ≥96% and DDH ~70%; thresholds proposed for species definition

338 (Lindsey et al., 2023)) while strain K4 and the bins represented three novel  
339 *Methanothermobacter* species (Fig. 2C).  
340 At the pan-genome level, the Marburg clade comprised 2076 gene clusters (GCs) with  
341 1564 (75.3%) forming the core genome (shared by all seven genomes), 324 (15.6%)  
342 constituting the accessory genome (specific to a subset of genomes) and 188 (9.1%)  
343 being unique to a single genome (Fig. 2C). The core genome contained the full suite for  
344 proteins encoded to carry out the hydrogenotrophic pathway. Members of this clade can  
345 assimilate acetyl-coA *via* the CO-methylating acetyl-CoA synthase from methyl-  
346 tetrahydromethanopterin. In strain Marburg, this complex was also shown to play a key  
347 role in CO oxidation (Diender et al., 2016). Moreover, the presence of all genes  
348 involved in carboxydutrophic methanogenesis in all Marburg clade genomes suggests  
349 they are also able to grow with CO as the sole carbon source. A protein of the carbonic  
350 anhydrase family (Cah), known to potentially convert bicarbonate into bioavailable  
351 CO<sub>2</sub>, was also present. Finally, as strains Clermont and Marburg were unable to grow  
352 on formate as an energy source (data not shown), the function of the formate  
353 dehydrogenase (FdhAB) is likely to reduce CO<sub>2</sub> to formate for its use in the purine  
354 synthesis (Kaster et al, 2011).

### 355 **3.3. Comparison of CH<sub>4</sub> yields between the pure cultures-strains Clermont and** 356 **Marburg-, and the mixed adapted culture**

#### 357 ***3.3.1. CH<sub>4</sub> yield during growth under reduced conditions***

358 The isolation of a new strain for the species *M. marburgensis* (strain Clermont) from a  
359 reactor microbiome enabled to compare CH<sub>4</sub> yield not only between two strains of the  
360 same species but also between strain Clermont and the community from which it was  
361 isolated. In this respect, a flow cytometry method based on the cofactor F420

362 fluorescence (Lambrecht et al., 2017) was used for quantification and each culture was  
363 inoculated with  $5.7 \times 10^5$  archaeal cells. The maximum specific growth rates ( $\mu_{MAX}$ )  
364 were 0.017, 0.03 and  $0.02 \text{ h}^{-1}$  for strain Clermont, Marburg and the mixed adapted  
365 culture, respectively.

366 Methanogenic activity was observed at one-day post-inoculation for strain Clermont  
367 and the mixed adapted culture (Fig. 3).  $\text{CH}_4$  yield increased linearly until total  $\text{H}_2$   
368 conversion, reaching a maximum value after six days of growth, corresponding to  
369  $54.3\% \pm 1.4\%$   $\text{CH}_4$  in the gas fraction for strain Clermont and to  $49.3\% \pm 2.6\%$  for the  
370 mixed adapted culture ( $p < 0.05$ ). This aligns with the view that the use of unique, self-  
371 replicating catalysts would avoid a loss of efficiency in biogas upgrading due to  $\text{H}_2$   
372 oxidation by other hydrogenotrophic microorganisms (Martin et al, 2013).

373 For strain Marburg, methanogenic activity was observed three days post-inoculation,  
374 *i.e.* with a two-day lag phase compared with strain Clermont. Total  $\text{H}_2$  conversion was  
375 observed after eight days of growth, resulting in a maximum of  $53.9\% \pm 2.4\%$   $\text{CH}_4$  in  
376 the gas fraction, a proportion similar to that obtained for strain Clermont (Fig. 3,  
377  $p > 0.05$ ). Consequently, the medium used in this study (*i.e.* BA medium), which is that  
378 used for the isolation of strain Clermont, favoured the growth behaviour of the latter but  
379 not its  $\text{CH}_4$  yield. As the two pure strains are genetically very close, one explanation of  
380 the two-day delay for strain Marburg may be, in part, attributed to their accessory  
381 genomes. Indeed, the genome of strain Clermont contains 121 genes that are not present  
382 in strain Marburg while the genome of strain Marburg contains 49 genes not found in  
383 strain Clermont, all mostly organized into clusters (the largest contained 34 genes for  
384 strain Clermont while 11 genes, for strain Marburg; See supplementary material).

385 Among these accessory genes, those encoding glycosyltransferases associated with the

386 synthesis and glycosylation of cellular surface proteins (*e.g* RafB, WcaA, WcaE) were  
387 more abundant in strain Clermont (See supplementary material). Kaster et al. (2011)  
388 suggested that these protein families might be partially responsible for the observed  
389 differences in growth rate phenotype between strain Marburg and *M.*  
390 *thermautotrophicus*. If this hypothesis proves to be true, it could also partly account for  
391 the observed phenotypic differences between strains Clermont and Marburg.

### 392 **3.3.2. CH<sub>4</sub> yield following oxidative stress**

393 As methanation reactors can experience episodic oxygenation (accidents, maintenance  
394 operations), it is essential to assess the HMs ability to maintain CH<sub>4</sub> yield after exposure  
395 to O<sub>2</sub>. This has never been done for *Methanothermobacter* species, either in pure or  
396 mixed cultures. Interestingly, the results showed that O<sub>2</sub> exposure had no impact on the  
397 pure strains (*i.e.* strains Clermont and Marburg) as they exhibited the same CH<sub>4</sub> yield  
398 levels when all H<sub>2</sub> was consumed (*e.g.* 51.2% ± 1.6% and 55.3% ± 2.3%, respectively;  
399 after 240 min of O<sub>2</sub> exposure, Fig. 4B), whatever the time of exposure to O<sub>2</sub>, *i.e* from 0  
400 min up to 240 min (p>0.05; See supplemental material). The O<sub>2</sub> resistance capacity of  
401 these strains is suspected to be mediated by the presence in their genome of energy-free  
402 reactive oxygen species (ROS) scavengers of various protection enzymes, *i.e.*  
403 superoxide dismutase (SOD), superoxide reductase (SOR), F<sub>420</sub>H<sub>20</sub> oxidase (FprA),  
404 peroxiredoxin (PRX), and rubrerythrin (Rbr) (Fig. 5), as previously reported for other  
405 methanogens (Liu et al., 2022). However, no catalase-encoding gene was found, similar  
406 to what was observed by Lyu and Lu (2018) in the Class I methanogens (*i.e.*  
407 *Methanobacteriales*, *Methanocellales* and *Methanopyrales*) to which  
408 *Methanothermobacter* spp. belongs. In all Marburg clade genomes, most ROS  
409 scavengers co-localize with genes encoding protection enzymes like rubredoxin (Rub,

410 electron providers to SOD and SOR), ferritin (FtnA, iron detoxifier during transient O<sub>2</sub>)  
411 (Fig. 5) and F390-synthetase which is thought to have a regulatory function in O<sub>2</sub> stress  
412 response (Vermeij et al., 1997). As most of these genes are up-regulated during the  
413 growth of strain Marburg on CO, it was hypothesized that they respond to redox stress  
414 in general, and not just to O<sub>2</sub> stress, or are regulated by universal stress proteins  
415 (Diender et al., 2016). Moreover, strain Marburg still shows the same two-day lag  
416 compared with strain Clermont. Its growth behaviour is therefore not altered by oxic  
417 stress either.

418 Conversely, exposure to O<sub>2</sub> has an impact on CH<sub>4</sub> yield by the mixed adapted culture.  
419 Indeed, it exhibited a slight increase from the sixth day of incubation, when all H<sub>2</sub> was  
420 converted, with 50.1% ± 1.6% CH<sub>4</sub> yield at 240 min of O<sub>2</sub> exposure (Fig. 4A) versus  
421 46.4% ± 2.9% at 0 min (p<0.02; See supplementary material), thereby reaching the  
422 level of the pure cultures (Fig. 4B). This gap in CH<sub>4</sub> yield could be associated with the  
423 inhibition of hydrogenotrophic microorganisms, other than strain Clermont, present in  
424 the mixed adapted culture.

425

#### 426 **4. Conclusions**

427 Although methanogenesis is well studied, gaps remain in the understanding of  
428 biomethanation, particularly regarding the choice between pure and mixed cultures in an  
429 energy bioprocess. Comparative analysis of bioenergetic performances between strain  
430 Clermont and its native consortium shows that the pure strain outperforms the  
431 consortium in CH<sub>4</sub> yield under reduced conditions. However, this is no longer the case  
432 after exposure to O<sub>2</sub>. Furthermore, although both pure strains show the same CH<sub>4</sub> yield,

433 strain Clermont displays a higher reaction speed than the type strain of its species under  
434 the culture conditions used in this study.

435

436 E-supplementary data of this work can be found in online version of the paper.

437

#### 438 **Data availability**

439 The raw reads of the 16S rRNA gene sequencing and genomic data were deposited at  
440 the NCBI database under the BioProject PRJNA1044399. *M. marburgensis* strain  
441 Clermont was deposited in the DSMZ German Collection of Microorganisms under  
442 accession number DSM 34405. Although the strain is not in the DSMZ catalogue or  
443 website, it is available on demand.

444

#### 445 **References**

- 446 Antunes, A, Rainey, F.A., Wanner, G., Taborda, M., Pätzold, J., Nobre, M.F., da Costa,  
447 M.S., Huber, R., 2008. A new lineage of halophilic, wall-less, contractile  
448 bacteria from a brine-filled deep of the Red Sea. *J. Bacteriol.* 190, 3580-3587.  
449 [https://doi.org/ 10.1128/JB.01860-07](https://doi.org/10.1128/JB.01860-07)
- 450 Bassani, I., Kougias, P.G., Treu, L., Angelidaki, I., 2015. Biogas Upgrading via  
451 Hydrogenotrophic Methanogenesis in Two-Stage Continuous Stirred Tank  
452 Reactors at Mesophilic and Thermophilic Conditions. *Environ. Sci. Technol.* 49,  
453 12585–12593. <https://doi.org/10.1021/acs.est.5b03451>
- 454 Bellini, R., Bassani, I., Vizzarro, A., Azim, A., Vasile, N., Pirri, C., Verga, F., Menin,  
455 B., 2022. Biological Aspects, Advancements and Techno-Economical



456 Evaluation of Biological Methanation for the Recycling and Valorization of  
457 CO<sub>2</sub>. *Energies* 15, 4064. <https://doi.org/10.3390/en15114064>

458 Biderre-Petit, C., Courtine, D., Hennequin, C., Galand, P.E., Bertilsson, S., Debroas, D.,  
459 Monjot, A., Lepère, C., Divne, A., Hochart, C., 2024. A pan-genomic approach  
460 reveals novel *Sulfurimonas* clade in the ferruginous meromictic Lake Pavin.  
461 *Mol. Ecol. Resour.* e13923. <https://doi.org/10.1111/1755-0998.13923>

462 Blanco, H., Nijs, W., Ruf, J., Faaij, A., 2018. Potential of Power-to-Methane in the EU  
463 energy transition to a low carbon system using cost optimization. *Appl. Energy*  
464 232, 323–340. <https://doi.org/10.1016/j.apenergy.2018.08.027>

465 Bokulich, N.A., Subramanian, S., Faith, J.J., Gevers, D., Gordon, J.I., Knight, R., Mills,  
466 D.A., Caporaso, J.G., 2013. Quality-filtering vastly improves diversity estimates  
467 from Illumina amplicon sequencing. *Nat. Methods* 10, 57–59.  
468 <https://doi.org/10.1038/nmeth.2276>

469 Braga Nan, L., Trably, E., Santa-Catalina, G., Bernet, N., Delgenès, J.-P., Escudié, R.,  
470 2020. Biomethanation processes: new insights on the effect of a high H<sub>2</sub> partial  
471 pressure on microbial communities. *Biotechnol. Biofuels* 13, 141.  
472 <https://doi.org/10.1186/s13068-020-01776-y>

473 Bu, F., Dong, N., Kumar Khanal, S., Xie, L., Zhou, Q., 2018. Effects of CO on  
474 hydrogenotrophic methanogenesis under thermophilic and extreme-thermophilic  
475 conditions: Microbial community and biomethanation pathways. *Bioresour.*  
476 *Technol.* 266, 364–373. <https://doi.org/10.1016/j.biortech.2018.03.092>

477 Burkhardt, M., Koschack, T., Busch, G., 2015. Biocatalytic methanation of hydrogen  
478 and carbon dioxide in an anaerobic three-phase system. *Bioresour. Technol.* 178,  
479 330–333. <https://doi.org/10.1016/j.biortech.2014.08.023>

480 Campanaro, S., Treu, L., Rodriguez-R, L.M., Kovalovszki, A., Ziels, R.M., Maus, I.,  
481 Zhu, X., Kougias, P.G., Basile, A., Luo, G., Schlüter, A., Konstantinidis, K.T.,  
482 Angelidaki, I., 2020. New insights from the biogas microbiome by  
483 comprehensive genome-resolved metagenomics of nearly 1600 species  
484 originating from multiple anaerobic digesters. *Biotechnol. Biofuels* 13, 25.  
485 <https://doi.org/10.1186/s13068-020-01679-y>

486 Carmona-Martínez, A.A., Trably, E., Milferstedt, K., Lacroix, R., Etcheverry, L.,  
487 Bernet, N., 2015. Long-term continuous production of H<sub>2</sub> in a microbial  
488 electrolysis cell (MEC) treating saline wastewater. *Water Res.* 81, 149–156.  
489 <https://doi.org/10.1016/j.watres.2015.05.041>

490 Chen, S., Zhou, Y., Chen, Y., Gu, J., 2018. fastp: an ultra-fast all-in-one FASTQ  
491 preprocessor. *Bioinformatics* 34, i884–i890.  
492 <https://doi.org/10.1093/bioinformatics/bty560>

493 Delmont, T.O., Eren, A.M., 2018. Linking pangenomes and metagenomes: the  
494 *Prochlorococcus* metapangenome. *PeerJ.* 6, e4320.  
495 <https://doi.org/10.7717/peerj.4320>

496 Diender, M., Pereira, R., Wessels, H.J.C.T., Stams, A.J.M., Sousa, D.Z., 2016.  
497 Proteomic Analysis of the Hydrogen and Carbon Monoxide Metabolism of  
498 *Methanothermobacter marburgensis*. *Front. Microbiol.* 7.  
499 <https://doi.org/10.3389/fmicb.2016.01049>

500 Glenk, G., Reichelstein, S., 2022. Reversible Power-to-Gas systems for energy  
501 conversion and storage. *Nat. Commun.* 13, 2010.  
502 <https://doi.org/10.1038/s41467-022-29520-0>

503 He, W., Yang, J., Jing, Y., Xu, L., Yu, K., Fang, X., 2023. NGenomeSyn: an easy-to-  
504 use and flexible tool for publication-ready visualization of syntenic relationships  
505 across multiple genomes. *Bioinformatics* 39, btad121.  
506 <https://doi.org/10.1093/bioinformatics/btad121>

507 Hungate, R.E., 1969. Chapter IV A Roll Tube Method for Cultivation of Strict  
508 Anaerobes, in: *Methods in Microbiology*. Elsevier, pp. 117–132.  
509 [https://doi.org/10.1016/S0580-9517\(08\)70503-8](https://doi.org/10.1016/S0580-9517(08)70503-8)

510 Kaster, A.-K., Goenrich, M., Seedorf, H., Liesegang, H., Wollherr, A., Gottschalk, G.,  
511 Thauer, R.K., 2011. More Than 200 Genes Required for Methane Formation  
512 from H<sub>2</sub> and CO<sub>2</sub> and Energy Conservation Are Present in  
513 *Methanothermobacter marburgensis* and *Methanothermobacter*  
514 *thermautotrophicus*. *Archaea* 2011, 1–23. <https://doi.org/10.1155/2011/973848>

515 Kaul, A., Böllmann, A., Thema, M., Kalb, L., Stöckl, R., Huber, H., Sterner, M.,  
516 Bellack, A., 2022. Combining a robust thermophilic methanogen and packing  
517 material with high liquid hold-up to optimize biological methanation in trickle-  
518 bed reactors. *Bioresour. Technol.* 345, 126524.  
519 <https://doi.org/10.1016/j.biortech.2021.126524>

520 Laguillaumie, L., Rafrafi, Y., Moya-Lecalir, E., Delagnes, D., Dubos, S., Spérandio,  
521 M., Paul, E., Dumas, C., 2022. Stability of ex situ biological methanation of  
522 H<sub>2</sub>/CO<sub>2</sub> with a mixed microbial culture in a pilot scale bubble column reactor.  
523 *Bioresour. Technol.* 354, 127180.  
524 <https://doi.org/10.1016/j.biortech.2022.127180>

525 Lambrecht, J., Cichocki, N., Hübschmann, T., Koch, C., Harms, H., Müller, S., 2017.  
526 Flow cytometric quantification, sorting and sequencing of methanogenic archaea

527 based on F420 autofluorescence. *Microb. Cell Factories* 16, 180.  
528 <https://doi.org/10.1186/s12934-017-0793-7>

529 Lindsey, R.L., Gladney, L.M., Huang, A.D., Griswold, T., Katz, L.S., Dinsmore, B.A.,  
530 Im, M.S., Kucerova, Z., Smith, P.A., Lane, C., Carleton, H.A., 2023. Rapid  
531 identification of enteric bacteria from whole genome sequences using average  
532 nucleotide identity metrics. *Front. Microbiol.* 14, 1225207.  
533 <https://doi.org/10.3389/fmicb.2023.1225207>

534 Liu, T., Li, X., Yekta, S.S., Björn, A., Mu, B.-Z., Masuda, L.S.M., Schnürer, A., Enrich-  
535 Prast, A., 2022. Absence of oxygen effect on microbial structure and methane  
536 production during drying and rewetting events. *Sci. Rep.* 12, 16570.  
537 <https://doi.org/10.1038/s41598-022-20448-5>

538 Lyu, Z., Lu, Y., 2018. Metabolic shift at the class level sheds light on adaptation of  
539 methanogens to oxidative environments. *ISME J.* 12, 411–423.  
540 <https://doi.org/10.1038/ismej.2017.173>

541 Martin, M., 2011. Cutadapt removes adapter sequences from high-throughput  
542 sequencing reads. *EMBnet.journal* 17, 10. <https://doi.org/10.14806/ej.17.1.200>

543 Martin, M.R., Fornero, J.J., Stark, R., Mets, L., Angenent, L.T., 2013. A Single-Culture  
544 Bioprocess of *Methanothermobacter thermautotrophicus* to Upgrade Digester  
545 Biogas by CO<sub>2</sub>-to-CH<sub>4</sub>. Conversion with H<sub>2</sub>. *Archaea* 2013, 1–11.  
546 <https://doi.org/10.1155/2013/157529>

547 Meier-Kolthoff, J.P., Auch, A.F., Klenk, H.-P., Göker, M., 2013. Genome sequence-  
548 based species delimitation with confidence intervals and improved distance  
549 functions. *BMC Bioinformatics* 14, 60. <https://doi.org/10.1186/1471-2105-14-60>

550 Minh, B.Q., Schmidt, H.A., Chernomor, O., Schrempf, D., Woodhams, M.D., Von  
551 Haeseler, A., Lanfear, R., 2020. IQ-TREE 2: New Models and Efficient  
552 Methods for Phylogenetic Inference in the Genomic Era. *Mol. Biol. Evol.* 37,  
553 1530–1534. <https://doi.org/10.1093/molbev/msaa015>

554 Nakagawa, S., Inagaki, F., Suzuki, Y., Steinsbu, B.O., Lever, M.A., Takai, K., Engelen,  
555 B., Sako, Y., Wheat, C.G., Horikoshi, K., Integrated Ocean Drilling Program  
556 Expedition 301 Scientists, 2006. Microbial Community in Black Rust Exposed  
557 to Hot Ridge Flank Crustal Fluids. *Appl. Environ. Microbiol.* 72, 6789–6799.  
558 <https://doi.org/10.1128/AEM.01238-06>

559 Paniagua, S., Lebrero, R., Muñoz, R., 2022. Syngas biomethanation: Current state and  
560 future perspectives. *Bioresour. Technol.* 358, 127436.  
561 <https://doi.org/10.1016/j.biortech.2022.127436>

562 Pruesse, E., Quast, C., Knittel, K., Fuchs, B.M., Ludwig, W., Peplies, J., Glockner,  
563 F.O., 2007. SILVA: a comprehensive online resource for quality checked and  
564 aligned ribosomal RNA sequence data compatible with ARB. *Nucleic Acids*  
565 *Res.* 35, 7188–7196. <https://doi.org/10.1093/nar/gkm864>

566 Pfeifer, K., Ergal, Í., Koller, M., Basen, M., Schuster, B., Rittmann, S.K.-M.R., 2021.  
567 *Archaea Biotechnology*. *Biotechnol. Adv.* 47, 107668.  
568 <https://doi.org/10.1016/j.biotechadv.2020.107668>

569 Rachbauer, L., Beyer, R., Bochmann, G., Fuchs, W., 2017. Characteristics of adapted  
570 hydrogenotrophic community during biomethanation. *Sci. Total Environ.* 595,  
571 912–919. <https://doi.org/10.1016/j.scitotenv.2017.03.074>

572 Rafrafi, Y., Laguillaumie, L., Dumas, C., 2021. Biological Methanation of H<sub>2</sub> and CO<sub>2</sub>  
573 with Mixed Cultures: Current Advances, Hurdles and Challenges. *Waste*

574 Biomass Valorization 12, 5259–5282. <https://doi.org/10.1007/s12649-020->  
575 01283-z

576 Rittmann, S.K.-M.R., Seifert, A.H., Bernacchi, S., 2018. Kinetics, multivariate  
577 statistical modelling, and physiology of CO<sub>2</sub>-based biological methane  
578 production. *Appl. Energy* 216, 751–760.  
579 <https://doi.org/10.1016/j.apenergy.2018.01.075>

580 Rognes, T., Flouri, T., Nichols, B., Quince, C., Mahé, F., 2016. VSEARCH: a versatile  
581 open source tool for metagenomics. *PeerJ* 4, e2584.  
582 <https://doi.org/10.7717/peerj.2584>

583 Seifert, A.H., Rittmann, S., Herwig, C., 2014. Analysis of process related factors to  
584 increase volumetric productivity and quality of biomethane with  
585 *Methanothermobacter marburgensis*. *Appl. Energy* 132, 155–162.  
586 <https://doi.org/10.1016/j.apenergy.2014.07.002>

587 Sun, W., Yu, G., Louie, T., Liu, T., Zhu, C., Xue, G., Gao, P., 2015. From mesophilic to  
588 thermophilic digestion: the transitions of anaerobic bacterial, archaeal, and  
589 fungal community structures in sludge and manure samples. *Appl. Microbiol.*  
590 *Biotechnol.* 99, 10271–10282. <https://doi.org/10.1007/s00253-015-6866-9>

591 Szuhaj, M., Wirth, R., Bagi, Z., Maróti, G., Rákhely, G., Kovács, K.L., 2021.  
592 Development of Stable Mixed Microbiota for High Yield Power to Methane  
593 Conversion. *Energies* 14, 7336. <https://doi.org/10.3390/en14217336>

594 Tang, Y.Q., Matsui, T., Morimura, S., Wu, X.L., Kida, K., 2008. Effect of Temperature  
595 on Microbial Community of a Glucose-Degrading Methanogenic Consortium  
596 under Hyperthermophilic Chemostat Cultivation. *J. BioSci. Bioeng.* 106, 180–  
597 187. <https://doi.org/10.1263/jbb.106.180>.

598 Thema, M., Weidlich, T., Kaul, A., Böllmann, A., Huber, H., Bellack, A., Karl, J.,  
599 Sterner, M., 2021. Optimized biological CO<sub>2</sub>-methanation with a pure culture of  
600 thermophilic methanogenic archaea in a trickle-bed reactor. *Bioresour. Technol.*  
601 333, 125135. <https://doi.org/10.1016/j.biortech.2021.125135>

602 Tong, D., Farnham, D.J., Duan, L., Zhang, Q., Lewis, N.S., Caldeira, K., Davis, S.J.,  
603 2021. Geophysical constraints on the reliability of solar and wind power  
604 worldwide. *Nat. Commun.* 12, 6146. [https://doi.org/10.1038/s41467-021-26355-](https://doi.org/10.1038/s41467-021-26355-z)  
605 [z](https://doi.org/10.1038/s41467-021-26355-z)

606 Treu, L., Kougias, P.G., De Diego-Díaz, B., Campanaro, S., Bassani, I., Fernández-  
607 Rodríguez, J., Angelidaki, I., 2018. Two-year microbial adaptation during  
608 hydrogen-mediated biogas upgrading process in a serial reactor configuration.  
609 *Bioresour. Technol.* 264, 140–147.  
610 <https://doi.org/10.1016/j.biortech.2018.05.070>

611 Tsapekos, P., Alvarado-Morales, M., Angelidaki, I., 2022. H<sub>2</sub> competition between  
612 homoacetogenic bacteria and methanogenic archaea during biomethantion from  
613 a combined experimental-modelling approach. *J. Environ. Chem. Eng.* 10,  
614 107281. <https://doi.org/10.1016/j.jece.2022.107281>

615 Vermeij, P., Pennings, J.L., Maassen, S.M., Keltjens, J.T., Vogels, G.D., 1997. Cellular  
616 levels of factor 390 and methanogenic enzymes during growth of  
617 *Methanobacterium thermoautotrophicum* deltaH. *J. Bacteriol.* 179, 6640–6648.  
618 <https://doi.org/10.1128/jb.179.21.6640-6648.1997>

619 Wahid, R., Mulat, D.G., Gaby J.C., Horn, S.V., 2019. Effects of H<sub>2</sub>:CO<sub>2</sub> ratio and H<sub>2</sub>  
620 supply fluctuation on methane content and microbial community composition

621 during *in-situ* biological biogas upgrading. *Biotechnol Biofuels* 12, 104.  
622 <https://doi.org/10.1186/s13068-019-1443-6>

623 Wick, R.R., Judd, L.M., Gorrie, C.L., Holt, K.E., 2017. Unicycler: Resolving bacterial  
624 genome assemblies from short and long sequencing reads. *PLOS Comput. Biol.*  
625 13, e1005595. <https://doi.org/10.1371/journal.pcbi.1005595>

626 Xu, J., Bu, F., Zhu, W., Luo, G., Xie, L., 2020. Microbial Consortiums of  
627 Hydrogenotrophic Methanogenic Mixed Cultures in Lab-Scale Ex-Situ Biogas  
628 Upgrading Systems under Different Conditions of Temperature, pH and CO.  
629 *Microorganisms* 8, 772. <https://doi.org/10.3390/microorganisms8050772>

630  
631



632 **Figure captions:**

633 **Figure 1: Relative abundance of microbial taxa inferred from Illumina MiSeq**

634 **sequencing of 16S rRNA genes. (A)** Archaeal abundance at the genus level from the

635 V4-V5 16S rRNA region of the 16S rRNA gene. The pie chart on right indicates

636 abundance of minor genera (<2% of total archaeal reads). **(B)** Bacterial abundance at

637 the phylum level from the V3-V4 16S rRNA region of the 16S rRNA gene. The pie

638 charts on right show the proportion of the different classes and genera constituting the

639 phyla *Bacillota* and *Pseudomonadota*.

640 **Figure 2: Comparative genomics of strain Clermont. (A)** Phylogenomic tree of

641 major archaeal clades based on a 73 genes core set using GToTree v1.8.2. **On left:**

642 Known major clades, including *Methanothermobacter* (dark pink) are collapsed and

643 shown as wedges of different colors. *Halobacteriales* was placed as outgroup. Bar, 0.3

644 substitution per amino acid position. **On right:** Decollapsed *Methanothermobacter*

645 wedge showing the position of strain Clermont (in red) within this genus. Bar, 0.05

646 substitution per amino acid position. **(B)** Collinearity analysis among assemblies of the

647 seven genomes forming the Marburg clade using MUMmer v4.0.0rc1 and visualized

648 using NGenomeSyn. **(C)** Anvi'o representation of the pan-genome of the Marburg

649 clade. Gene clusters (n = 2076) were ordered according to a hierarchical clustering of

650 their presence/absence (inner dendrogram). Rings show the presence (filled) or absence

651 (undashed) of the gene clusters in each genome. Single copy core and other core: gene

652 clusters present in all seven *Methanothermobacter* genomes. Gene clusters exclusively

653 present in a unique genome are indicated by a number: 1. strain K4, 2. strain THM\_2, 3.

654 JZ-3\_D\_bin\_25, 4. strain Kepco-1, 5. GMQ\_75\_MeOH\_H2\_bin\_21, 6. strain Marburg,

655 7. strain Clermont. To the right is given an ANI percentage identity heatmap; red: 100%  
656 identity; light red: values ranging from 96% to 97%; white: values <96%.

657 **Figure 3: Methane yield under reduced conditions in batch culture for pure strains**  
658 **(i.e. Marburg and Clermont) and the mixed adapted culture.** An asterisk denotes a  
659 significant difference ( $p < 0.05$ ) between strain Marburg versus the two other cultures  
660 (days 3 to 6), and between the mixed culture versus pure cultures (days 8 and 18). The  
661 error bar indicates the standard error (n=3).

662 **Figure 4: Methane yield in batch cultures under oxidative stressed conditions (240**  
663 **min of exposure to O<sub>2</sub>).** (A) Comparison over time between strain Clermont and mixed  
664 adapted culture. (B) Comparison over time between strain Clermont and strain Marburg.  
665 An asterisk denotes a significant difference ( $p < 0.05$ ) between cultures over time. The  
666 error bar indicates the standard error (n=3).

667 **Figure 5: Schematic representation of oxidative stress protection enzymes detected**  
668 **in the Marburg clade genomes.** (A) Gene-loci in the genome of strain Marburg. (B)  
669 Potential cellular responses to oxidative stress.

670  
671

1       1   **Title**

2  
3       2   Comparison of methane yield of a novel strain of *Methanothermobacter marburgensis*  
4  
5       3   in pure and mixed adapted culture derived from a methanation bubble column  
6  
7  
8       4   bioreactor  
9

10  
11       5  
12  
13       6   **Abstract**

14  
15       7   The ongoing discussion regarding the use of mixed or pure cultures of  
16  
17  
18       8   hydrogenotrophic methanogenic archaea in Power-to-Methane (P2M) bioprocess  
19  
20       9   applications persists, with each option presenting its own advantages and disadvantages.  
21  
22       10  To address this issue, a comparison of methane (CH<sub>4</sub>) yield between a novel  
23  
24       11  methanogenic archaeon belonging to the species *Methanothermobacter marburgensis*  
25  
26       12  (strain Clermont) isolated from a biological methanation column, and the community  
27  
28       13  from which it originated, was conducted. This comparison included the type strain *M.*  
29  
30       14  *marburgensis* str. Marburg. The evaluation also examined how exposure to oxygen (O<sub>2</sub>)  
31  
32       15  for up to 240 minutes impacted the CH<sub>4</sub> yield across these cultures. While both  
33  
34       16  *Methanothermobacter* strains exhibit comparable CH<sub>4</sub> yield, slightly higher than that of  
35  
36       17  the mixed adapted culture under non-O<sub>2</sub>-exposed conditions, strain Clermont does not  
37  
38       18  display the lag time observed for strain Marburg.  
39  
40  
41  
42  
43  
44  
45  
46

47       19  
48       20  **Keywords**

49       21  *Methanothermobacter marburgensis*, mixed hydrogenotrophic methanogenic culture,  
50  
51       22  oxygen exposure, multi-omics approaches.  
52  
53

54       23  
55  
56  
57       24  **1. Introduction**  
58  
59  
60  
61  
62  
63  
64  
65

1 25 To limit the rise of global surface temperature to less than 2°C while meeting the  
2  
3  
4 26 increasing energy demand, a significant global energy transition is urgently needed.  
5  
6 27 However, shifting away from polluting fossil fuels to low-carbon solutions requires  
7  
8 28 technological innovation, particularly in renewable energy. Despite substantial progress  
9  
10 29 in wind, solar, and geothermal energies, challenges such as intermittency, variability,  
11  
12 30 geographical limitations, and storage persist (Tong et al., 2021). Power-To-Gas (P2G)  
13  
14 31 concept has emerged as a promising solution allowing the storage of surplus of  
15  
16 32 renewable energy recovered from the electricity sector in the form of gas (*i.e.*  
17  
18 33 dihydrogen (H<sub>2</sub>) called P2H and CH<sub>4</sub> called P2M) (Glenk and Reichelstein, 2022).  
19  
20  
21  
22 34 Currently, P2M offers advantages over P2H. It allows converting electricity into  
23  
24 35 chemical energy and uses existing infrastructure. Considering storability, it has a higher  
25  
26 36 energy density (10 kWh/Nm<sup>3</sup> for CH<sub>4</sub> versus 3 kWh/Nm<sup>3</sup> for H<sub>2</sub>) and is suitable for  
27  
28 37 long term and large-scale storage (Blanco et al., 2018). P2M systems combine H<sub>2</sub>  
29  
30 38 oxidation and carbon dioxide (CO<sub>2</sub>) reduction to produce CH<sub>4</sub> using either  
31  
32 39 physicochemical or biological catalysts (biomethanation). Comparatively,  
33  
34 40 biomethanation processes require lower temperatures and pressures than  
35  
36 41 physicochemical methanation processes and exhibit increased resistance to chemical  
37  
38 42 contaminants including hydrogen sulfide (H<sub>2</sub>S), organic acids, or ammonia (Burkhardt  
39  
40 43 et al., 2015).  
41  
42 44 Hydrogenotrophic methanogenic archaea (HMs), which can use H<sub>2</sub> as a reducing agent  
43  
44 45 for the conversion of CO<sub>2</sub> into CH<sub>4</sub>, are key biocatalysts for biomethane (Bellini et al.,  
45  
46 46 2022). They require as much H<sub>2</sub> as the system can provide for CO<sub>2</sub> reduction.  
47  
48 47 Therefore, the competition and sustainable equilibrium between H<sub>2</sub> producers (*e.g.*  
49  
50 48 acetogens) and consumers (*e.g.* HMs) usually result in a very low dissolved H<sub>2</sub> partial  
51  
52  
53  
54  
55  
56  
57  
58  
59  
60  
61  
62  
63  
64  
65

1 49 pressure ( $p(\text{H}_2)$ ) to maintain a balanced operation of the entire microbiological  
2  
3 50 community. However, numerous abiotic and biotic factors can affect this equilibrium.  
4  
5 51 From a thermodynamical perspective, external  $\text{H}_2$  provision strongly favours  
6  
7 52 hydrogenotrophic methanogenesis. But a sudden increment of  $p(\text{H}_2)$  can enable the  
8  
9 53 homoacetogenic pathway to outcompete the hydrogenotrophic methanogenesis (Treu et  
10  
11 54 al., 2018; Tsapekos et al., 2022). In addition, temperature, pH,  $\text{H}_2/\text{CO}_2$  ratio,  $\text{H}_2$  supply,  
12  
13 55 etc, are all abiotic factors that can influence  $\text{CH}_4$  content and microbial community  
14  
15 56 during *in-situ* biological biogas upgrading (Rachbauer et al., 2017; Wahid et al., 2019).  
16  
17 57 Among HMs, the main actors in biomethanation processes comprise members of the  
18  
19 58 genera *Methanoculleus*, *Methanothermobacter*, *Methanobacterium*, or *Methanosarcina*.  
20  
21 59 The relative abundance of these genera in biogas upgrading reactors varies based on  
22  
23 60 factors such as temperature, pH, carbon monoxide (CO), etc (Thema et al., 2021; Xu et  
24  
25 61 al., 2020). In thermophilic conditions, *Methanothermobacter* was shown to be  
26  
27 62 predominant in the mixed cultures due to its favorable growth at higher temperatures  
28  
29 63 (Kaster et al., 2011; Szuhaj et al., 2021). Within this genus, *Methanothermobacter*  
30  
31 64 *thermautotrophicus* and *Methanothermobacter marburgensis*, largely used as model  
32  
33 65 organisms, have already been implemented as biocatalysts in large-scale industrial  
34  
35 66 processes because they are robust, and reach high cell densities, and  $\text{CH}_4$  production  
36  
37 67 rate (Seifert et al., 2014; Pfeifer et al., 2021; Thema et al., 2021, Kaul et al., 2022).  
38  
39 68 Two main approaches can be employed for biomethanation, *i.e.* using pure cultures or  
40  
41 69 enriched mixed cultures, each with its own advantages and drawbacks (Rachbauer et al.,  
42  
43 70 2017; Rafrafi et al., 2021; Rittmann et al., 2018). Indeed, using single self-replicating  
44  
45 71 catalysts would prevent oxidation of  $\text{H}_2$  by other hydrogenotrophic microorganisms,  
46  
47 72 thereby avoiding a loss of efficiency in biogas upgrading. It would also allow for better  
48  
49  
50  
51  
52  
53  
54  
55  
56  
57  
58  
59  
60  
61  
62  
63  
64  
65

1 73 system variability and behaviour prediction (Martin et al., 2013). On the other hand,  
2  
3 74 using consortia would be more efficient, leading to larger CH<sub>4</sub> yields (Bellini et al,  
4  
5 75 2022, Paniagua et al., 2022). Other advantages of employing consortia include greater  
6  
7 76 robustness and short recovery time upon starvation/excess input gas rate and  
8  
9 77 oxygenation. However, managing mixed cultures often requires increased control and a  
10  
11 78 thorough understanding of how microbial composition impacts the system (Paniagua et  
12  
13 79 al., 2022). Therefore, despite the growing number of studies in this field, the question of  
14  
15 80 whether pure or mixed cultures are more suitable for biomethanation processes remains  
16  
17 81 unresolved. To address this question, a comparison of the performance of both HM pure  
18  
19 82 cultures and reactor microbiomes from which HMs have been isolated appears essential.  
20  
21 83 This study aims to evaluate the methanation efficiency of a new HM affiliated to the *M.*  
22  
23 84 *marburgensis* species (strain Clermont) isolated from a bubble column reactor. Its  
24  
25 85 methanogenic performance was compared not only with its native consortium but also  
26  
27 86 with the type strain, *i.e.* *M. marburgensis* strain Marburg (hereinafter referred to as  
28  
29 87 strain Marburg). This comparison was extended under oxidative stress, a common  
30  
31 88 occurrence in biomethanation processes.  
32  
33  
34  
35  
36  
37  
38  
39  
40

## 41 90 **2. Material and Methods**

### 42 91 **2.1. Laboratory-scale methanation reactor**

43 92 The mixed adapted culture used in this study was collected from a 3.5 L bubble column  
44  
45 93 reactor, six weeks after its inoculation with 300 mL of digestate from a thermophilic  
46  
47 94 industrial-scale biogas plant treating livestock effluent and agri-food industry wastes  
48  
49 95 that operates between 52 and 54°C (Methelec, Ennezat, France). Briefly, the reactor  
50  
51 96 contained 2.7 L of basal anaerobic (BA) culture medium prepared as previously  
52  
53 97 reported (Bu et al., 2018) and reduced by introducing 0.4 g/L of sodium sulfide  
54  
55  
56  
57  
58  
59  
60  
61  
62  
63  
64  
65

1 98 nanohydrate ( $\text{Na}_2\text{S}\cdot 9\text{H}_2\text{O}$ ). The  $\text{H}_2/\text{CO}_2$  gas mixture was set at a ratio of 4:1 (v/v) with a  
2  
3  
4 99 mass flowmeter (SLA5800, Brooks Instrument, Hatfield, USA). Flow rates ranged from  
5  
6 100 0.29 to 0.44  $\text{NL}\cdot\text{min}^{-1}$ . The temperature was set to  $55^\circ\text{C}$  using a thermostatic bath (Eco  
7  
8 101 RE1225 silver, Lauda, Königshofen, Germany).

9  
10  
11 102 Volatile fatty acids (VFAs) in the six-week mixed adapted culture were determined  
12  
13 103 using a liquid chromatograph (1260 HPLC, Agilent, Santa Clara, USA). The HPLC  
14  
15 104 apparatus was equipped with two columns (Rezex ROA 300 x 7.8 nm, Phenomenex,  
16  
17 105 Torrance, USA) mounted in serial in an oven ( $50^\circ\text{C}$ ) and coupled with a refractive index  
18  
19  
20 106 detector. The mobile phase was a 2 mM sulfuric acid in ultra-pure water pumped at 0.7  
21  
22 107  $\text{mL}\cdot\text{min}^{-1}$  and 70 bars. For the analysis, 2 mL of sample were mixed with 125  $\mu\text{L}$  of  
23  
24 108  $\text{Ba}(\text{OH})_2\cdot 8\text{H}_2\text{O}$  (0.3 M) and 125  $\mu\text{L}$  of  $\text{ZnSO}_4\cdot 7\text{H}_2\text{O}$  (5% w/v) before a 5 min  
25  
26 109 centrifugation at 10000 g. Samples were filtered through 0.2  $\mu\text{m}$  nylon filters before  
27  
28 110 being injected in the HPLC apparatus.

29  
30  
31 111 Measurements of archaeal and bacterial abundance (quantitative real-time PCR),  
32  
33 112 performed on the six-week sample mixed adapted culture, revealed a dominance of  
34  
35 113 archaea over bacteria with an archaea/bacteria ratio of five ( $1.0\ 10^9$  archaeal cells/mL  
36  
37 114 versus  $2.2\ 10^8$  bacterial cells/mL).

## 38 115 **2.2. Microbial community analysis of the mixed adapted culture**

39  
40  
41 116 Two mL of the six-week mixed adapted culture were centrifuged at 10000 g at room  
42  
43 117 temperature (RT) for 10 min and total genomic DNA (gDNA) was extracted from the  
44  
45 118 pellet using a Nucleo Spin Soil kit in accordance with manufacturer's instructions  
46  
47 119 (Machery Nagel, Düren, Germany). Then, gDNA was quantified using a  
48  
49 120 spectrophotometer (NanoDrop 1000, Thermo Fisher Scientific, USA). Subsequently,  
50  
51 121 the V3-V4 hypervariable region of the bacterial 16S ribosomal RNA (rRNA) genes was  
52  
53  
54  
55  
56  
57  
58  
59  
60  
61  
62  
63  
64  
65

1 122 amplified using the primer set F343 (5'-  
2  
3 123 CTTTCCCTACACGACGCTCTTCCGATCTACGGRAGGCAGCAG-3') - R784 (5'-  
4  
5 124 GGAGTTCAGACGTGTGCTCTTCCGATCTTACCAGGGTATCTAATCCT-3')  
6  
7  
8 125 (Carmona-Martinez et al., 2015) while the V4-V5 region of the archaeal 16S rRNA  
9  
10 126 genes was amplified with the primer set F504-519 (5'-  
11  
12 127 CTTTCCCTACACGACGCTCTTCCGATCTCAGCMGCCGCGGKAA-3') and R910-  
13  
14 128 928 (5'-GGAGTTCAGACGTGTGCTCTTCCGATCTCCCGCCWATTCCTTTAAGT-  
15  
16 129 3') (Braga Nan et al., 2020), primers containing adapters and barcodes for Miseq  
17  
18 130 sequencing. PCR reactions contained Taq<sup>TM</sup> TaKaRa Premix, 1 µM of each primer, 200  
19  
20 131 µM of each deoxynucleoside triphosphate (dNTP), 0.625 U TaKaRa Taq polymerase  
21  
22 132 (TakaRa Inc., France), nuclease free-H<sub>2</sub>O and 50 to 100 ng gDNA template in a total  
23  
24 133 volume of 50 µL. For both bacteria and archaea, after a denaturation step of 1 min at  
25  
26 134 98°C, PCR steps at 98°C for 1 min, 59°C for 40 s, and 72°C for 1 min were repeated 35  
27  
28 135 times, followed by an elongation step at 72°C for 10 min in a Mastercycler® thermal  
29  
30 136 cyclor (Eppendorf, Hamburg, Germany). Amplicon size was checked by Agilent High  
31  
32 137 Sensitivity DNA Kit on 2100 Bioanalyzer (Agilent Technologies, Santa Clara, CA,  
33  
34 138 USA). Amplicon libraries were prepared and sequenced by the GenoToul platform  
35  
36 139 (Toulouse, France) with an Illumina MiSeq sequencer to generate 2 x 300 bp paired-end  
37  
38 140 reads. Bacterial and archaeal reads were separately processed using a homemade  
39  
40 141 bioinformatics pipeline. Briefly, paired reads were merged using the VSEARCH  
41  
42 142 v2.18.0 (Rognes et al., 2016) and then trimmed and filtered with Cutadapt (Martin,  
43  
44 143 2011) to minimize the effects of random sequencing errors as follows: (i) only merged  
45  
46 144 reads with a length 200-500 bp were kept, (ii) paired reads with sequencing errors in  
47  
48 145 primers were discarded and (iii) primer sequences and nucleotides with Phred quality  
49  
50  
51  
52  
53  
54  
55  
56  
57  
58  
59  
60  
61  
62  
63  
64  
65



1 146 scores upper than 30 were trimmed. Deletion of chimeric sequences and clusterization  
2  
3 147 were carried out using VSEARCH (Rognes et al., 2016) and operational taxonomic  
4  
5 148 units (OTUs) that accounted for <0.005% of the total set of sequences were discarded  
6  
7  
8 149 (Bokulich et al., 2013). The taxonomic assignment was performed against the SILVA  
9  
10 150 v138.1 SSU NR99 database using the global alignment script in VSEARCH (Pruesse et  
11  
12  
13 151 al, 2007; Rognes et al., 2016).

### 152 **2.3. Hydrogenotrophic methanogenic archaea isolation and analytical procedures**

153 A serum vial (Dutscher, Bernolsheim, France) containing 50 ml of BA medium (110  
19  
20 154 mL in capacity) was inoculated with an aliquot of the six-week mixed adapted culture  
21  
22 155 (10% v/v). After BA medium autoclaving, and prior to its inoculation, dinitrogen (N<sub>2</sub>)  
23  
24 156 filling the head space was replaced by H<sub>2</sub>/CO<sub>2</sub> (4:1, v/v) gas mixture from a gas  
25  
26  
27 157 cylinder (Westfalen, France) at 2 bars. Liquid cultivation was conducted at 55°C in the  
28  
29 158 dark, without agitation.

30  
31 159 HM isolation was performed *via* successive dilution to extinction series in Hungate  
32  
33 160 tubes (16.5 mL capacity) containing 5 mL of either liquid or solid BA medium (2% agar  
34  
35 161 w/v; roll-tube technique (Hungate, 1969)). Headspace composition was determined by  
36  
37 162 gas chromatography (3000A MicroGC, Agilent Technologies, Santa Clara, CA, USA)  
38  
39  
40 163 equipped with two capillary columns (one MS-5A column associated with a backflush  
41  
42 164 injector and one PorapLOT Q column associated with a standard injector) and Soprane  
43  
44  
45 165 software v3.5.2 for the analysis. The microGC used argon as gas carrier and the  
46  
47  
48 166 temperature of the columns and injectors were at 50 and 60°C, respectively.

49  
50  
51 167 The purity of HMs was checked by microscopic observations (Leica DM IRB inverted  
52  
53 168 microscope equipped with a Hamamatsu C13440 camera and Zen Blue v3.1 software)  
54  
55  
56 169 and by adding yeast extract (2 g/L) and glucose (20 mM final concentration) to the BA  
57  
58  
59  
60  
61  
62  
63  
64  
65

1 170 medium to confirm the absence of fermentative bacteria. Subsequently, HM taxonomic  
2  
3 171 identification was performed by 16S rRNA gene sequence amplification using the  
4  
5 172 universal primer set Arch21F-1492R (Nakagawa et al., 2006) followed by sequencing  
6  
7 173 (Eurofins Genomics, Cologne, Germany). For the ultrastructural characterization, the  
8  
9 174 archaeal cells in 1% (v/v) formaldehyde fixed samples were collected by centrifugation  
10  
11 175 at 20000 g for 20 min at 14°C directly onto 400-mesh electron microscopy copper grids  
12  
13 176 covered with carbon-coated Formvar film (AO3X, Pelanne Instruments, Toulouse,  
14  
15 177 France). Particles were over contrasted with 2% uranyl salts and rinsed three times in  
16  
17 178 distilled deionized water before being dried at RT. Subsequently, the characterization  
18  
19 179 was performed with a transmission electron microscope using a JEOL 2100  
20  
21 180 (Akishikma, Tokyo, Japan; Plateforme CYSTEM, UCA Partner, Clermont-Ferrand,  
22  
23 181 France). The microscope was operated at 80 kV, and the images were recorded with an  
24  
25 182 Gatan CMOS RIO 9 camera (Gatan Ametek, Pleasanton, USA) at 3072 x 3072 pixels.  
26  
27 183 Since all HMs belonged to the same strain, one representative, called  
28  
29 184 *Methanothermobacter marburgensis* strain Clermont (hereafter referred to as strain  
30  
31 185 Clermont), was deposited in the Deutsche Sammlung von Mikroorganismen und  
32  
33 186 Zellkulturen (DSMZ) culture collection (accession number DSM 34405).

#### 187 **2.4. Cultivation procedures**

188 The hydrogenotrophic and methanogenic activities of strain Clermont, the mixed  
189 adapted culture, and *M. marburgensis* strain Marburg obtained from DSMZ (DSM  
190 2133), which is the closest relative of strain Clermont (99.5% 16S rRNA gene identity),  
191 were investigated under reduced conditions. Cultures were conducted in serum vials  
192 containing 50 mL of BA medium as described above (Paragraph 2.3). All inoculations  
193 were performed with the same number of archaeal cells, *i.e.*  $5.7 \times 10^5$  cells. Briefly, an

1 194 aliquot of 1 mL of pure or mixed cultures at the end of the exponential growth phase  
2  
3  
4 195 was diluted to 1:10 and directly used for flow cytometry analysis (BD LSR Fortessa X-  
5  
6 196 20; BD Biosciences, CA, USA). Two lasers (Violet, 405 nm, 50 mW and Blue, 488 nm,  
7  
8 197 60 mW) were used for F420 cofactor excitation (autofluorescence of archaeal cells) and  
9  
10 198 morphological characterization, respectively. The threshold was set at 200 on the F420  
11  
12 199 cofactor parameter. Data were acquired during 60 sec at a constant flow rate of 29.85  
13  
14 200  $\mu\text{L}/\text{min}$  and processed using FACSDivA 9 software (BD Biosciences).  
15  
16 201 Cultures subjected to oxidative stress were inoculated and grown in medium devoid of  
17  
18 202 chemical reducing agents, namely  $\text{Na}_2\text{S}\cdot 9\text{H}_2\text{O}$  and resazurin, generally used to reinforce  
19  
20 203 anaerobiosis and detect any potential oxidation, to prevent  $\text{O}_2$  reduction during the  
21  
22 204 exposure. Indeed, their presence would have reduced the effective amount of  $\text{O}_2$  during  
23  
24 205 oxic stress. Anaerobiosis prior to oxic stress was confirmed by microGC. After reaching  
25  
26 206 the end of the exponential growth phase in anaerobic conditions, the cultures were  
27  
28 207 transferred to sterile beakers in a laminar flow hood and placed under high stirring  
29  
30 208 speed to be exposed to atmospheric levels of  $\text{O}_2$  (21%) for durations of 0, 10, 30, 60, 90,  
31  
32 209 120, and 240 min. The quantity of dissolved  $\text{O}_2$  measured in the medium was  $10 \text{ mg}/\text{L} \pm$   
33  
34 210  $0.32 \text{ mg}/\text{L}$  from 1 min up to 240 min of exposure (portable oximeter, Laqua 200 series,  
35  
36 211 Horiba Scientific, Japan). Subsequently, fresh BA medium containing a reducing agent  
37  
38 212 was inoculated as above. The absence of  $\text{O}_2$  was checked by gas chromatography before  
39  
40 213 incubation.  
41  
42 214 All experiments were conducted in biological triplicates. During growth, gas  
43  
44 215 composition in the headspace was monitored daily by gas chromatography. Statistical  
45  
46 216 analysis of  $\text{CH}_4$  yield during growth was conducted using the Student t-test, one-way or  
47  
48 217 two-way ANOVA (culture  $\times$  incubation days) followed by Tukey's test under normality  
49  
50  
51  
52  
53  
54  
55  
56  
57  
58  
59  
60  
61  
62  
63  
64  
65

1 218 and homoscedasticity assumption. The level of significance was set at  $\alpha=0.05$ . All  
2  
3 219 statistical analyses were performed using the R Stats package v4.2.2.  
4

## 5 220 **2.5. DNA extraction for whole genome sequencing of the *M. marburgensis* strain**

### 6 221 **Clermont**

7  
8 222 A culture of strain Clermont (50 mL) in exponential growth was concentrated by  
9  
10  
11 223 centrifugation for 15 min at 10000 g at RT. gDNA was extracted from the pellet using a  
12  
13 224 standard phenol–chloroform method (Biderre-Petit et al, 2024) before quantification on  
14  
15 225 a Qubit Fluorometer (ThermoFisher Scientific, USA) by using Qubit™ dsDNA HS  
16  
17 226 assay kit in accordance with manufacturer’s instructions. Subsequently, 300 ng of  
18  
19 227 gDNA were sequenced using Illumina HiSeq technology (2 × 150 bp; Eurofins  
20  
21 228 Genomics, Constance, Germany). Raw paired-end reads were quality-filtered with fastp  
22  
23 229 v0.23.4 (Chen et al., 2018). *De novo* assembly of whole genome sequencing data was  
24  
25 230 performed using Unicycler v0.5.0 (Wick et al., 2017) with default settings. In the  
26  
27 231 following step, the short contigs with viral/transposable elements (BLASTX search  
28  
29 232 against non-redundant database) and fragmented rRNA operons (barrnap v0.9 and  
30  
31 233 parameter "--kingdom arc", <https://github.com/tseemann/barrnap>) were filtered out.  
32  
33  
34  
35  
36  
37  
38  
39

## 40 234 **2.6. Phylogenomic tree construction**

41  
42 235 Representative genomes of *Methanothermobacterium*, *Methanonatronarchaeia*,  
43  
44 236 *Archaeoglobi*, *Methanobacteria*, *Methanococci*, *Methanomicrobia*, *Methanopyri*,  
45  
46 237 *Thermococci*, and *Halobacterium* were downloaded from the National Center for  
47  
48 238 Biotechnology Information (NCBI) RefSeq. Subsequently, a genome-based  
49  
50 239 phylogenetic tree was generated with the program GToTree v1.8.2 as reported in  
51  
52 240 Biderre-Petit et al. (2024), using an archaea-specific gene set composed of 73 markers.  
53  
54  
55 241 Individual gene alignments were concatenated to construct a species tree using IQ-  
56  
57  
58  
59  
60  
61  
62  
63  
64  
65

1 242 TREE v2.2.3 with the evolution model LG+F+I+R10 and parameters "-B 2000 --alrt  
2  
3 243 2000 --bnni" (Minh et al., 2020). *Halobacterium* was used as an outgroup.

## 4 244 **2.7. Pan-genomic analysis and other genome characterizations**

5  
6 245 Pan-genomic analysis of the Marburg clade (*i.e.* including the strains Marburg,  
7  
8 246 Clermont and their closest relatives-strain KEPCO-1 (assembly accession  
9  
10 247 GCA\_008033705.1), strain K4 (GCA\_022014235.1), strain THM2  
11  
12 248 (GCA\_009917665.1), bin GMQ\_75\_MeOH\_H2\_bin\_21 (GCA\_030055425.1) and bin  
13  
14 249 JZ-3\_D\_bin\_25 (GCA\_030055435.1); seven genomes in total) was carried out using the  
15  
16 250 "pan-genomics workflow of anvi'o v7.1 (Delmont and Eren, 2018). The average  
17  
18 251 nucleotide identity (ANI) was also calculated through anvi'o and to complete the  
19  
20 252 results, *in silico* DNA-DNA hybridization (*isDDH*) was computed using Genome-to-  
21  
22 253 Genome Distance Calculator v2.1 with formula 2 as previously recommended (Meier-  
23  
24 254 Kolthoff et al., 2013). Genome synteny was visualized by NGenomeSyn v1.41 (He et  
25  
26 255 al., 2023).

## 27 256 28 29 257 **3. Results and discussion**

### 30 258 **3.1. Overview of microbial community diversity in a bubble column reactor**

31 259 Metabarcoding procedure was used to separately address the archaeal and bacterial  
32  
33 260 diversity present in the six-week adapted culture. Although less abundant than archaea,  
34  
35 261 bacteria showed much higher diversity, with 833 OTUs (19403 reads in total) versus 42  
36  
37 262 OTUs (28482 reads), respectively, which is consistent with what is generally described  
38  
39 263 for mixed cultures (Xu et al., 2020). For the archaea, the four most abundant OTUs  
40  
41 264 (>1% relative abundance in the sample) covered 96.1% of the community (See  
42  
43 265 supplementary material). *Methanothermobacter* genus represented 98.5% of the  
44  
45  
46  
47  
48  
49  
50  
51  
52  
53  
54  
55  
56  
57  
58  
59  
60  
61  
62  
63  
64  
65

1 266 archaeal community in terms of reads, followed by *Methanobacterium* (1.2%),  
2  
3 267 *Methanomassiliicoccus* (0.09%) and *Methanoculleus* (0.01%) (Fig. 1A). This finding  
4  
5 268 closely aligns with previous research, which has shown that *Methanothermobacter* is  
6  
7  
8 269 the dominant genus in the hydrogenotrophic methanogenic consortium of *ex-situ*  
9  
10 270 methanation systems at 55°C (Xu et al., 2020). Within this genus, 98.9% of the reads  
11  
12 271 are affiliated to the *M. marburgensis* species (>97% 16S rRNA gene sequence identity).  
13  
14 272 Regarding bacteria, the most represented phyla in terms of reads were *Bacillota* (ex  
15  
16 273 *Firmicutes*, 91.8% of total bacterial reads) followed by *Pseudomonadota* (ex  
17  
18 274 *Proteobacteria*, 6.8%) (Fig. 1B), in agreement with previous studies (Bassani et al.,  
19  
20 275 2015; Campanaro et al., 2020). The 11 most abundant OTUs (>1% relative abundance  
21  
22 276 in the sample) covered 48.7% of the bacterial community (See supplementary material)  
23  
24 277 and mostly affiliated with the genus *Haloplasma* (35.2% of all bacterial reads) and the  
25  
26 278 class *Limnochordia* (33.2%) in *Bacillota*.  
27  
28 279 The most abundant taxon, *i.e.* *Haloplasma*, is currently represented by only one  
29  
30 280 representative, a halophilic bacterium isolated from a deep-sea brine lake, named *H.*  
31  
32 281 *contractile*. The growth limit of this bacterium was determined at 44°C (Antunes et al,  
33  
34 282 2008), which is not in accordance with the temperature used in this study, *i.e.* 55°C.  
35  
36 283 However, although SILVA classifies this predominant taxon in the genus *Haloplasma*,  
37  
38 284 the sequence used as reference and which shows 99% identity with OTUs affiliated to  
39  
40 285 *Haloplasma* (accession number FN436037, see supplementary material), displays only  
41  
42 286 up to 89% sequence similarity with *Haloplasma* using BLAST N against the nucleotide  
43  
44 287 database in NCBI. This may be due to the low number of sequences representative of  
45  
46 288 the genus *Haloplasma* and also more generally of the family and order. Indeed, the  
47  
48 289 order Haloplasmatales currently includes a single family -Haloplasmataceae- which  
49  
50  
51  
52  
53  
54  
55  
56  
57  
58  
59  
60  
61  
62  
63  
64  
65

1 290 includes a single genus and species: *H. contractile*. This most likely not only leads to an  
2  
3  
4 291 inaccurate affiliation at the genus level, but also potentially at the family level.  
5  
6 292 Consequently, the representatives that will be discovered for this group of  
7  
8 293 Haloplasmatales will most certainly allow significant changes to the current description  
9  
10 294 made for the single type species.  
11  
12 295 The second most abundant taxon, the *Limnochordia* class, is frequently observed in full-  
13  
14 296 size and laboratory-scale thermophilic biogas reactors (Campanaro et al., 2020). The  
15  
16 297 main representative in this class was MBA03 (14.6% of all bacterial reads).  
17  
18 298 Laguillaumie et al. (2022) suggested that MBA03, referenced as a carbohydrate  
19  
20 299 fermentative taxon, would grow on lysis products and prevent side products, such as  
21  
22 300 VFAs, from accumulating in the reactor. The low amount of VFAs measured in the  
23  
24 301 reactor could therefore be explained, at least in part, by the MBA03 abundance. This  
25  
26 302 low quantity also indicates that hydrogenotrophic methanogenesis has not shifted  
27  
28 303 towards homoacetogenesis. Moreover, MBA03 association with *Methanobacterium* was  
29  
30 304 described as an indicator of process stability (Laguillaumie et al., 2022). Its association  
31  
32 305 with *Methanothermobacter* could therefore still be such an indicator.  
33  
34 306 In addition to MBA03, two other bacteria known to be syntrophic acetate oxidizing, *i.e.*  
35  
36 307 *Tepidiphilus* (*Pseudomonadota*) and norank order D8A-2 (*Bacillota*), showed  
37  
38 308 significant relative abundance, with 2.9% and 3.6% of all bacterial reads, respectively.  
39  
40 309 These results are in line with previous studies, which showed that these taxa were  
41  
42 310 abundant in thermophilic samples and worked synergistically with HMs, providing the  
43  
44 311 substrates they need towards biogas production (Tang et al., 2008; Xu et al., 2020). An  
45  
46 312 anaerobic digestion system seeded from manure samples (which is comparable to what  
47  
48 313 was used for the bioreactor, *i.e.* a biogas plant treating livestock effluent) and running at  
49  
50  
51  
52  
53  
54  
55  
56  
57  
58  
59  
60  
61  
62  
63  
64  
65

1 314 55°C (Sun et al., 2015), was shown to be populated with similar microbial taxa. This  
2  
3 315 supports the view that temperature, but also inoculum, are crucial variables in  
4  
5 316 determining the structure of microbial consortia in hydrogenotrophic methanogenic  
6  
7 317 mixed cultures (Xu et al., 2020).  
8  
9

### 10 318 **3.2. Isolation and genome sequencing of *M. marburgensis* strain Clermont**

11 319 The strain isolated from the bioreactor belonged to the genus *Methanothermobacter* and  
12  
13 320 showed >99.5% identity with strain Marburg 16S rRNA gene sequence (accession  
14  
15 321 number NR\_102881.1). It was named *M. marburgensis* strain Clermont and deposited  
16  
17 322 in the DSMZ collection (DSM 34405). This strain was rod-shaped (~5 µm long and 0.6  
18  
19 323 µm wide) and non-motile (See supplementary material).  
20  
21  
22

23 324 The draft genome of strain Clermont (~330-fold coverage), featuring six contigs (from  
24  
25 325 ~21.9 to 776.9 kb), had a total length of ~1.72 Mb, a N50 contig length of 593 kb, and  
26  
27 326 a G+C content of 48.7%. The number of coding DNA sequences was 1805 with two  
28  
29 327 16S-23S rRNA gene clusters, three 5S rRNA genes and 37 transfer RNA (tRNA) genes.  
30  
31 328 No extra-chromosomal genetic elements were detected. Genome fragmentation was  
32  
33 329 mainly due to the high conservation degree between rRNA operons and transposase  
34  
35 330 sequences that hamper the assembly tool to resolve these loci. Phylogenomic analysis  
36  
37 331 confirmed the close relationship of strain Clermont with strain Marburg but also with  
38  
39 332 three other *Methanothermobacter* strains (*i.e.* KEPCO-1, THM\_2, and K4) and two bins  
40  
41 333 (*i.e.* GMQ\_75\_MeOH\_H2\_bin\_21 and JZ-3\_D\_bin\_25). They all formed a clade  
42  
43 334 (hereinafter referred to as Marburg clade) within the genus *Methanothermobacter* (Fig.  
44  
45 335 2A). Their genomes revealed a high degree of synteny (Fig. 2B). Based on ANI and  
46  
47 336 *is*DDH values, strains Clermont, Marburg, KEPCO\_1 and THM\_2 formed a single  
48  
49 337 species (ANI ≥96% and DDH ~70%; thresholds proposed for species definition  
50  
51  
52  
53  
54  
55  
56  
57  
58  
59  
60  
61  
62  
63  
64  
65



1 338 (Lindsey et al., 2023)) while strain K4 and the bins represented three novel  
2  
3 339 *Methanothermobacter* species (Fig. 2C).  
4  
5 340 At the pan-genome level, the Marburg clade comprised 2076 gene clusters (GCs) with  
6  
7 341 1564 (75.3%) forming the core genome (shared by all seven genomes), 324 (15.6%)  
8  
9 342 constituting the accessory genome (specific to a subset of genomes) and 188 (9.1%)  
10  
11 343 being unique to a single genome (Fig. 2C). The core genome contained the full suite for  
12  
13 344 proteins encoded to carry out the hydrogenotrophic pathway. Members of this clade can  
14  
15 345 assimilate acetyl-coA *via* the CO-methylating acetyl-CoA synthase from methyl-  
16  
17 346 tetrahydromethanopterin. In strain Marburg, this complex was also shown to play a key  
18  
19 347 role in CO oxidation (Diender et al., 2016). Moreover, the presence of all genes  
20  
21 348 involved in carboxydrotrophic methanogenesis in all Marburg clade genomes suggests  
22  
23 349 they are also able to grow with CO as the sole carbon source. A protein of the carbonic  
24  
25 350 anhydrase family (Cah), known to potentially convert bicarbonate into bioavailable  
26  
27 351 CO<sub>2</sub>, was also present. Finally, as strains Clermont and Marburg were unable to grow  
28  
29 352 on formate as an energy source (data not shown), the function of the formate  
30  
31 353 dehydrogenase (FdhAB) is likely to reduce CO<sub>2</sub> to formate for its use in the purine  
32  
33 354 synthesis (Kaster et al, 2011).  
34  
35

### 355 **3.3. Comparison of CH<sub>4</sub> yields between the pure cultures-strains Clermont and** 36 **Marburg-, and the mixed adapted culture**

#### 357 ***3.3.1. CH<sub>4</sub> yield during growth under reduced conditions***

358 The isolation of a new strain for the species *M. marburgensis* (strain Clermont) from a  
359 reactor microbiome enabled to compare CH<sub>4</sub> yield not only between two strains of the  
360 same species but also between strain Clermont and the community from which it was  
361 isolated. In this respect, a flow cytometry method based on the cofactor F420

1 362 fluorescence (Lambrecht et al., 2017) was used for quantification and each culture was  
2  
3 363 inoculated with  $5.7 \times 10^5$  archaeal cells. The maximum specific growth rates ( $\mu_{MAX}$ )  
4  
5 364 were 0.017, 0.03 and  $0.02 \text{ h}^{-1}$  for strain Clermont, Marburg and the mixed adapted  
6  
7  
8 365 culture, respectively.  
9  
10 366 Methanogenic activity was observed at one-day post-inoculation for strain Clermont  
11  
12 367 and the mixed adapted culture (Fig. 3).  $\text{CH}_4$  yield increased linearly until total  $\text{H}_2$   
13  
14 368 conversion, reaching a maximum value after six days of growth, corresponding to  
15  
16 369  $54.3\% \pm 1.4\%$   $\text{CH}_4$  in the gas fraction for strain Clermont and to  $49.3\% \pm 2.6\%$  for the  
17  
18 370 mixed adapted culture ( $p < 0.05$ ). This aligns with the view that the use of unique, self-  
19  
20 371 replicating catalysts would avoid a loss of efficiency in biogas upgrading due to  $\text{H}_2$   
21  
22 372 oxidation by other hydrogenotrophic microorganisms (Martin et al, 2013).  
23  
24 373 For strain Marburg, methanogenic activity was observed three days post-inoculation,  
25  
26 374 *i.e.* with a two-day lag phase compared with strain Clermont. Total  $\text{H}_2$  conversion was  
27  
28 375 observed after eight days of growth, resulting in a maximum of  $53.9\% \pm 2.4\%$   $\text{CH}_4$  in  
29  
30 376 the gas fraction, a proportion similar to that obtained for strain Clermont (Fig. 3,  
31  
32 377  $p > 0.05$ ). Consequently, the medium used in this study (*i.e.* BA medium), which is that  
33  
34 378 used for the isolation of strain Clermont, favoured the growth behaviour of the latter but  
35  
36 379 not its  $\text{CH}_4$  yield. As the two pure strains are genetically very close, one explanation of  
37  
38 380 the two-day delay for strain Marburg may be, in part, attributed to their accessory  
39  
40 381 genomes. Indeed, the genome of strain Clermont contains 121 genes that are not present  
41  
42 382 in strain Marburg while the genome of strain Marburg contains 49 genes not found in  
43  
44 383 strain Clermont, all mostly organized into clusters (the largest contained 34 genes for  
45  
46 384 strain Clermont while 11 genes, for strain Marburg; See supplementary material).  
47  
48 385 Among these accessory genes, those encoding glycosyltransferases associated with the  
49  
50  
51  
52  
53  
54  
55  
56  
57  
58  
59  
60  
61  
62  
63  
64  
65

1 386 synthesis and glycosylation of cellular surface proteins (*e.g* RafB, WcaA, WcaE) were  
2  
3 387 more abundant in strain Clermont (See supplementary material). Kaster et al. (2011)  
4  
5 388 suggested that these protein families might be partially responsible for the observed  
6  
7 389 differences in growth rate phenotype between strain Marburg and *M.*  
8  
9  
10 390 *thermautotrophicus*. If this hypothesis proves to be true, it could also partly account for  
11  
12 391 the observed phenotypic differences between strains Clermont and Marburg.  
13  
14

### 15 392 **3.3.2. CH<sub>4</sub> yield following oxidative stress**

16  
17  
18 393 As methanation reactors can experience episodic oxygenation (accidents, maintenance  
19  
20 394 operations), it is essential to assess the HMs ability to maintain CH<sub>4</sub> yield after exposure  
21  
22 395 to O<sub>2</sub>. This has never been done for *Methanothermobacter* species, either in pure or  
23  
24 396 mixed cultures. Interestingly, the results showed that O<sub>2</sub> exposure had no impact on the  
25  
26 397 pure strains (*i.e.* strains Clermont and Marburg) as they exhibited the same CH<sub>4</sub> yield  
27  
28 398 levels when all H<sub>2</sub> was consumed (*e.g.* 51.2% ± 1.6% and 55.3% ± 2.3%, respectively;  
29  
30 399 after 240 min of O<sub>2</sub> exposure, Fig. 4B), whatever the time of exposure to O<sub>2</sub>, *i.e* from 0  
31  
32 400 min up to 240 min (p>0.05; See supplemental material). The O<sub>2</sub> resistance capacity of  
33  
34 401 these strains is suspected to be mediated by the presence in their genome of energy-free  
35  
36 402 reactive oxygen species (ROS) scavengers of various protection enzymes, *i.e.*  
37  
38 403 superoxide dismutase (SOD), superoxide reductase (SOR), F<sub>420</sub>H<sub>20</sub> oxidase (FprA),  
39  
40 404 peroxiredoxin (PRX), and rubrerythrin (Rbr) (Fig. 5), as previously reported for other  
41  
42 405 methanogens (Liu et al., 2022). However, no catalase-encoding gene was found, similar  
43  
44 406 to what was observed by Lyu and Lu (2018) in the Class I methanogens (*i.e.*  
45  
46 407 *Methanobacteriales*, *Methanocellales* and *Methanopyrales*) to which  
47  
48 408 *Methanothermobacter* spp. belongs. In all Marburg clade genomes, most ROS  
49  
50 409 scavengers co-localize with genes encoding protection enzymes like rubredoxin (Rub,  
51  
52  
53  
54  
55  
56  
57  
58  
59  
60  
61  
62  
63  
64  
65

1 410 electron providers to SOD and SOR), ferritin (FtnA, iron detoxifier during transient O<sub>2</sub>)  
2  
3 411 (Fig. 5) and F390-synthetase which is thought to have a regulatory function in O<sub>2</sub> stress  
4  
5 412 response (Vermeij et al., 1997). As most of these genes are up-regulated during the  
6  
7 413 growth of strain Marburg on CO, it was hypothesized that they respond to redox stress  
8  
9 414 in general, and not just to O<sub>2</sub> stress, or are regulated by universal stress proteins  
10  
11 415 (Diender et al., 2016). Moreover, strain Marburg still shows the same two-day lag  
12  
13 416 compared with strain Clermont. Its growth behaviour is therefore not altered by oxic  
14  
15 417 stress either.

16  
17  
18 418 Conversely, exposure to O<sub>2</sub> has an impact on CH<sub>4</sub> yield by the mixed adapted culture.  
19  
20 419 Indeed, it exhibited a slight increase from the sixth day of incubation, when all H<sub>2</sub> was  
21  
22 420 converted, with 50.1% ± 1.6% CH<sub>4</sub> yield at 240 min of O<sub>2</sub> exposure (Fig. 4A) versus  
23  
24 421 46.4% ± 2.9% at 0 min (p<0.02; See supplementary material), thereby reaching the  
25  
26 422 level of the pure cultures (Fig. 4B). This gap in CH<sub>4</sub> yield could be associated with the  
27  
28 423 inhibition of hydrogenotrophic microorganisms, other than strain Clermont, present in  
29  
30 424 the mixed adapted culture.  
31  
32  
33  
34  
35  
36

37 425

#### 38 426 **4. Conclusions**

39  
40  
41 427 Although methanogenesis is well studied, gaps remain in the understanding of  
42  
43 428 biometanation, particularly regarding the choice between pure and mixed cultures in an  
44  
45 429 energy bioprocess. Comparative analysis of bioenergetic performances between strain  
46  
47 430 Clermont and its native consortium shows that the pure strain outperforms the  
48  
49 431 consortium in CH<sub>4</sub> yield under reduced conditions. However, this is no longer the case  
50  
51 432 after exposure to O<sub>2</sub>. Furthermore, although both pure strains show the same CH<sub>4</sub> yield,  
52  
53  
54  
55  
56  
57  
58  
59  
60  
61  
62  
63  
64  
65

1 433 strain Clermont displays a higher reaction speed than the type strain of its species under  
2  
3 434 the culture conditions used in this study.

4  
5  
6 435

7  
8 436 E-supplementary data of this work can be found in online version of the paper.

9  
10  
11 437

### 12 438 **Data availability**

13  
14  
15 439 The raw reads of the 16S rRNA gene sequencing and genomic data were deposited at

16  
17  
18 440 the NCBI database under the BioProject PRJNA1044399. *M. marburgensis* strain

19  
20  
21 441 Clermont was deposited in the DSMZ German Collection of Microorganisms under

22  
23 442 accession number DSM 34405. Although the strain is not in the DSMZ catalogue or

24  
25 443 website, it is available on demand.

26  
27  
28 444

### 29 445 **References**

30  
31  
32 446 Antunes, A, Rainey, F.A., Wanner, G., Taborda, M., Pätzold, J., Nobre, M.F., da Costa,

33  
34  
35 447 M.S., Huber, R., 2008. A new lineage of halophilic, wall-less, contractile

36  
37 448 bacteria from a brine-filled deep of the Red Sea. *J. Bacteriol.* 190, 3580-3587.

38  
39  
40 449 [https://doi.org/ 10.1128/JB.01860-07](https://doi.org/10.1128/JB.01860-07)

41  
42 450 Bassani, I., Kougias, P.G., Treu, L., Angelidaki, I., 2015. Biogas Upgrading via

43  
44 451 Hydrogenotrophic Methanogenesis in Two-Stage Continuous Stirred Tank

45  
46 452 Reactors at Mesophilic and Thermophilic Conditions. *Environ. Sci. Technol.* 49,

47  
48  
49 453 12585–12593. <https://doi.org/10.1021/acs.est.5b03451>

50  
51  
52 454 Bellini, R., Bassani, I., Vizzarro, A., Azim, A., Vasile, N., Pirri, C., Verga, F., Menin,

53  
54  
55 455 B., 2022. Biological Aspects, Advancements and Techno-Economical

56  
57  
58  
59  
60  
61  
62  
63  
64  
65

1 456 Evaluation of Biological Methanation for the Recycling and Valorization of  
2  
3 457 CO<sub>2</sub>. *Energies* 15, 4064. <https://doi.org/10.3390/en15114064>  
4  
5  
6 458 Biderre-Petit, C., Courtine, D., Hennequin, C., Galand, P.E., Bertilsson, S., Debroas, D.,  
7  
8 459 Monjot, A., Lepère, C., Divne, A., Hochart, C., 2024. A pan-genomic approach  
9  
10 460 reveals novel *Sulfurimonas* clade in the ferruginous meromictic Lake Pavin.  
11  
12 461 *Mol. Ecol. Resour.* e13923. <https://doi.org/10.1111/1755-0998.13923>  
13  
14  
15 462 Blanco, H., Nijs, W., Ruf, J., Faaij, A., 2018. Potential of Power-to-Methane in the EU  
16  
17 463 energy transition to a low carbon system using cost optimization. *Appl. Energy*  
18  
19 464 232, 323–340. <https://doi.org/10.1016/j.apenergy.2018.08.027>  
20  
21  
22 465 Bokulich, N.A., Subramanian, S., Faith, J.J., Gevers, D., Gordon, J.I., Knight, R., Mills,  
23  
24 466 D.A., Caporaso, J.G., 2013. Quality-filtering vastly improves diversity estimates  
25  
26 467 from Illumina amplicon sequencing. *Nat. Methods* 10, 57–59.  
27  
28 468 <https://doi.org/10.1038/nmeth.2276>  
29  
30  
31 469 Braga Nan, L., Trably, E., Santa-Catalina, G., Bernet, N., Delgenès, J.-P., Escudié, R.,  
32  
33 470 2020. Biomethanation processes: new insights on the effect of a high H<sub>2</sub> partial  
34  
35 471 pressure on microbial communities. *Biotechnol. Biofuels* 13, 141.  
36  
37 472 <https://doi.org/10.1186/s13068-020-01776-y>  
38  
39  
40 473 Bu, F., Dong, N., Kumar Khanal, S., Xie, L., Zhou, Q., 2018. Effects of CO on  
41  
42 474 hydrogenotrophic methanogenesis under thermophilic and extreme-thermophilic  
43  
44 475 conditions: Microbial community and biomethanation pathways. *Bioresour.*  
45  
46 476 *Technol.* 266, 364–373. <https://doi.org/10.1016/j.biortech.2018.03.092>  
47  
48  
49 477 Burkhardt, M., Koschack, T., Busch, G., 2015. Biocatalytic methanation of hydrogen  
50  
51 478 and carbon dioxide in an anaerobic three-phase system. *Bioresour. Technol.* 178,  
52  
53 479 330–333. <https://doi.org/10.1016/j.biortech.2014.08.023>  
54  
55  
56  
57  
58  
59  
60  
61  
62  
63  
64  
65

1 480 Campanaro, S., Treu, L., Rodriguez-R, L.M., Kovalovszki, A., Ziels, R.M., Maus, I.,  
2  
3  
4 481 Zhu, X., Kougias, P.G., Basile, A., Luo, G., Schlüter, A., Konstantinidis, K.T.,  
5  
6 482 Angelidaki, I., 2020. New insights from the biogas microbiome by  
7  
8 483 comprehensive genome-resolved metagenomics of nearly 1600 species  
9  
10  
11 484 originating from multiple anaerobic digesters. *Biotechnol. Biofuels* 13, 25.  
12  
13 485 <https://doi.org/10.1186/s13068-020-01679-y>  
14  
15  
16 486 Carmona-Martínez, A.A., Trably, E., Milferstedt, K., Lacroix, R., Etcheverry, L.,  
17  
18 487 Bernet, N., 2015. Long-term continuous production of H<sub>2</sub> in a microbial  
19  
20 488 electrolysis cell (MEC) treating saline wastewater. *Water Res.* 81, 149–156.  
21  
22 489 <https://doi.org/10.1016/j.watres.2015.05.041>  
23  
24  
25  
26 490 Chen, S., Zhou, Y., Chen, Y., Gu, J., 2018. fastp: an ultra-fast all-in-one FASTQ  
27  
28 491 preprocessor. *Bioinformatics* 34, i884–i890.  
29  
30 492 <https://doi.org/10.1093/bioinformatics/bty560>  
31  
32  
33 493 Delmont, T.O., Eren, A.M., 2018. Linking pangenomes and metagenomes: the  
34  
35 494 *Prochlorococcus* metapangenome. *PeerJ.* 6, e4320.  
36  
37 495 <https://doi.org/10.7717/peerj.4320>  
38  
39  
40 496 Diender, M., Pereira, R., Wessels, H.J.C.T., Stams, A.J.M., Sousa, D.Z., 2016.  
41  
42 497 Proteomic Analysis of the Hydrogen and Carbon Monoxide Metabolism of  
43  
44 498 *Methanothermobacter marburgensis*. *Front. Microbiol.* 7.  
45  
46 499 <https://doi.org/10.3389/fmicb.2016.01049>  
47  
48  
49  
50 500 Glenk, G., Reichelstein, S., 2022. Reversible Power-to-Gas systems for energy  
51  
52 501 conversion and storage. *Nat. Commun.* 13, 2010.  
53  
54 502 <https://doi.org/10.1038/s41467-022-29520-0>  
55  
56  
57  
58  
59  
60  
61  
62  
63  
64  
65

1 503 He, W., Yang, J., Jing, Y., Xu, L., Yu, K., Fang, X., 2023. NGenomeSyn: an easy-to-  
2  
3 504 use and flexible tool for publication-ready visualization of syntenic relationships  
4  
5 505 across multiple genomes. *Bioinformatics* 39, btad121.  
6  
7 506 <https://doi.org/10.1093/bioinformatics/btad121>  
8  
9  
10 507 Hungate, R.E., 1969. Chapter IV A Roll Tube Method for Cultivation of Strict  
11  
12 508 Anaerobes, in: *Methods in Microbiology*. Elsevier, pp. 117–132.  
13  
14 509 [https://doi.org/10.1016/S0580-9517\(08\)70503-8](https://doi.org/10.1016/S0580-9517(08)70503-8)  
15  
16  
17 510 Kaster, A.-K., Goenrich, M., Seedorf, H., Liesegang, H., Wollherr, A., Gottschalk, G.,  
18  
19 511 Thauer, R.K., 2011. More Than 200 Genes Required for Methane Formation  
20  
21 512 from H<sub>2</sub> and CO<sub>2</sub> and Energy Conservation Are Present in  
22  
23 513 *Methanothermobacter marburgensis* and *Methanothermobacter*  
24  
25 514 *thermautotrophicus*. *Archaea* 2011, 1–23. <https://doi.org/10.1155/2011/973848>  
26  
27  
28  
29 515 Kaul, A., Böllmann, A., Thema, M., Kalb, L., Stöckl, R., Huber, H., Sterner, M.,  
30  
31 516 Bellack, A., 2022. Combining a robust thermophilic methanogen and packing  
32  
33 517 material with high liquid hold-up to optimize biological methanation in trickle-  
34  
35 518 bed reactors. *Bioresour. Technol.* 345, 126524.  
36  
37 519 <https://doi.org/10.1016/j.biortech.2021.126524>  
38  
39  
40  
41 520 Laguillaumie, L., Rafrafi, Y., Moya-Lecalir, E., Delagnes, D., Dubos, S., Spérandio,  
42  
43 521 M., Paul, E., Dumas, C., 2022. Stability of ex situ biological methanation of  
44  
45 522 H<sub>2</sub>/CO<sub>2</sub> with a mixed microbial culture in a pilot scale bubble column reactor.  
46  
47 523 *Bioresour. Technol.* 354, 127180.  
48  
49 524 <https://doi.org/10.1016/j.biortech.2022.127180>  
50  
51  
52  
53 525 Lambrecht, J., Cichocki, N., Hübschmann, T., Koch, C., Harms, H., Müller, S., 2017.  
54  
55 526 Flow cytometric quantification, sorting and sequencing of methanogenic archaea  
56  
57  
58  
59  
60  
61  
62  
63  
64  
65



1 527 based on F420 autofluorescence. *Microb. Cell Factories* 16, 180.  
2  
3 528 <https://doi.org/10.1186/s12934-017-0793-7>  
4  
5  
6 529 Lindsey, R.L., Gladney, L.M., Huang, A.D., Griswold, T., Katz, L.S., Dinsmore, B.A.,  
7  
8 530 Im, M.S., Kucerova, Z., Smith, P.A., Lane, C., Carleton, H.A., 2023. Rapid  
9  
10 531 identification of enteric bacteria from whole genome sequences using average  
11  
12 532 nucleotide identity metrics. *Front. Microbiol.* 14, 1225207.  
13  
14 533 <https://doi.org/10.3389/fmicb.2023.1225207>  
15  
16  
17  
18 534 Liu, T., Li, X., Yekta, S.S., Björn, A., Mu, B.-Z., Masuda, L.S.M., Schnürer, A., Enrich-  
19  
20 535 Prast, A., 2022. Absence of oxygen effect on microbial structure and methane  
21  
22 536 production during drying and rewetting events. *Sci. Rep.* 12, 16570.  
23  
24 537 <https://doi.org/10.1038/s41598-022-20448-5>  
25  
26  
27  
28 538 Lyu, Z., Lu, Y., 2018. Metabolic shift at the class level sheds light on adaptation of  
29  
30 539 methanogens to oxidative environments. *ISME J.* 12, 411–423.  
31  
32 540 <https://doi.org/10.1038/ismej.2017.173>  
33  
34  
35 541 Martin, M., 2011. Cutadapt removes adapter sequences from high-throughput  
36  
37 542 sequencing reads. *EMBnet.journal* 17, 10. <https://doi.org/10.14806/ej.17.1.200>  
38  
39  
40 543 Martin, M.R., Fornero, J.J., Stark, R., Mets, L., Angenent, L.T., 2013. A Single-Culture  
41  
42 544 Bioprocess of *Methanothermobacter thermautotrophicus* to Upgrade Digester  
43  
44 545 Biogas by CO<sub>2</sub>-to-CH<sub>4</sub>. Conversion with H<sub>2</sub>. *Archaea* 2013, 1–11.  
45  
46 546 <https://doi.org/10.1155/2013/157529>  
47  
48  
49  
50 547 Meier-Kolthoff, J.P., Auch, A.F., Klenk, H.-P., Göker, M., 2013. Genome sequence-  
51  
52 548 based species delimitation with confidence intervals and improved distance  
53  
54 549 functions. *BMC Bioinformatics* 14, 60. <https://doi.org/10.1186/1471-2105-14-60>  
55  
56  
57  
58  
59  
60  
61  
62  
63  
64  
65

1 550 Minh, B.Q., Schmidt, H.A., Chernomor, O., Schrempf, D., Woodhams, M.D., Von  
2  
3 551 Haeseler, A., Lanfear, R., 2020. IQ-TREE 2: New Models and Efficient  
4  
5 552 Methods for Phylogenetic Inference in the Genomic Era. *Mol. Biol. Evol.* 37,  
6  
7 553 1530–1534. <https://doi.org/10.1093/molbev/msaa015>  
8  
9 554 Nakagawa, S., Inagaki, F., Suzuki, Y., Steinsbu, B.O., Lever, M.A., Takai, K., Engelen,  
10  
11 555 B., Sako, Y., Wheat, C.G., Horikoshi, K., Integrated Ocean Drilling Program  
12  
13 556 Expedition 301 Scientists, 2006. Microbial Community in Black Rust Exposed  
14  
15 557 to Hot Ridge Flank Crustal Fluids. *Appl. Environ. Microbiol.* 72, 6789–6799.  
16  
17 558 <https://doi.org/10.1128/AEM.01238-06>  
18  
19 559 Paniagua, S., Lebrero, R., Muñoz, R., 2022. Syngas biomethanation: Current state and  
20  
21 560 future perspectives. *Bioresour. Technol.* 358, 127436.  
22  
23 561 <https://doi.org/10.1016/j.biortech.2022.127436>  
24  
25 562 Pruesse, E., Quast, C., Knittel, K., Fuchs, B.M., Ludwig, W., Peplies, J., Glockner,  
26  
27 563 F.O., 2007. SILVA: a comprehensive online resource for quality checked and  
28  
29 564 aligned ribosomal RNA sequence data compatible with ARB. *Nucleic Acids*  
30  
31 565 *Res.* 35, 7188–7196. <https://doi.org/10.1093/nar/gkm864>  
32  
33 566 Pfeifer, K., Ergal, Í., Koller, M., Basen, M., Schuster, B., Rittmann, S.K.-M.R., 2021.  
34  
35 567 *Archaea Biotechnology. Biotechnol. Adv.* 47, 107668.  
36  
37 568 <https://doi.org/10.1016/j.biotechadv.2020.107668>  
38  
39 569 Rachbauer, L., Beyer, R., Bochmann, G., Fuchs, W., 2017. Characteristics of adapted  
40  
41 570 hydrogenotrophic community during biomethanation. *Sci. Total Environ.* 595,  
42  
43 571 912–919. <https://doi.org/10.1016/j.scitotenv.2017.03.074>  
44  
45 572 Rafrafi, Y., Laguillaumie, L., Dumas, C., 2021. Biological Methanation of H<sub>2</sub> and CO<sub>2</sub>  
46  
47 573 with Mixed Cultures: Current Advances, Hurdles and Challenges. *Waste*

1 574 Biomass Valorization 12, 5259–5282. <https://doi.org/10.1007/s12649-020->  
2  
3 575 01283-z  
4  
5  
6 576 Rittmann, S.K.-M.R., Seifert, A.H., Bernacchi, S., 2018. Kinetics, multivariate  
7  
8 577 statistical modelling, and physiology of CO<sub>2</sub>-based biological methane  
9  
10 578 production. *Appl. Energy* 216, 751–760.  
11  
12 579 <https://doi.org/10.1016/j.apenergy.2018.01.075>  
13  
14  
15 580 Rognes, T., Flouri, T., Nichols, B., Quince, C., Mahé, F., 2016. VSEARCH: a versatile  
16  
17 581 open source tool for metagenomics. *PeerJ* 4, e2584.  
18  
19 582 <https://doi.org/10.7717/peerj.2584>  
20  
21  
22 583 Seifert, A.H., Rittmann, S., Herwig, C., 2014. Analysis of process related factors to  
23  
24 584 increase volumetric productivity and quality of biomethane with  
25  
26 585 *Methanothermobacter marburgensis*. *Appl. Energy* 132, 155–162.  
27  
28 586 <https://doi.org/10.1016/j.apenergy.2014.07.002>  
29  
30  
31 587 Sun, W., Yu, G., Louie, T., Liu, T., Zhu, C., Xue, G., Gao, P., 2015. From mesophilic to  
32  
33 588 thermophilic digestion: the transitions of anaerobic bacterial, archaeal, and  
34  
35 589 fungal community structures in sludge and manure samples. *Appl. Microbiol.*  
36  
37 590 *Biotechnol.* 99, 10271–10282. <https://doi.org/10.1007/s00253-015-6866-9>  
38  
39  
40 591 Szuhaj, M., Wirth, R., Bagi, Z., Maróti, G., Rákhely, G., Kovács, K.L., 2021.  
41  
42 592 Development of Stable Mixed Microbiota for High Yield Power to Methane  
43  
44 593 Conversion. *Energies* 14, 7336. <https://doi.org/10.3390/en14217336>  
45  
46  
47 594 Tang, Y.Q., Matsui, T., Morimura, S., Wu, X.L., Kida, K., 2008. Effect of Temperature  
48  
49 595 on Microbial Community of a Glucose-Degrading Methanogenic Consortium  
50  
51 596 under Hyperthermophilic Chemostat Cultivation. *J. BioSci. Bioeng.* 106, 180–  
52  
53 597 187. <https://doi.org/10.1263/jbb.106.180>.  
54  
55  
56  
57  
58  
59  
60  
61  
62  
63  
64  
65

- 1 598 Thema, M., Weidlich, T., Kaul, A., Böllmann, A., Huber, H., Bellack, A., Karl, J.,  
2  
3 599 Sterner, M., 2021. Optimized biological CO<sub>2</sub>-methanation with a pure culture of  
4  
5 600 thermophilic methanogenic archaea in a trickle-bed reactor. *Bioresour. Technol.*  
6  
7 601 333, 125135. <https://doi.org/10.1016/j.biortech.2021.125135>  
8  
9  
10 602 Tong, D., Farnham, D.J., Duan, L., Zhang, Q., Lewis, N.S., Caldeira, K., Davis, S.J.,  
11  
12 603 2021. Geophysical constraints on the reliability of solar and wind power  
13  
14 604 worldwide. *Nat. Commun.* 12, 6146. <https://doi.org/10.1038/s41467-021-26355->  
15  
16 605 [z](https://doi.org/10.1038/s41467-021-26355-)  
17  
18  
19  
20 606 Treu, L., Kougias, P.G., De Diego-Díaz, B., Campanaro, S., Bassani, I., Fernández-  
21  
22 607 Rodríguez, J., Angelidaki, I., 2018. Two-year microbial adaptation during  
23  
24 608 hydrogen-mediated biogas upgrading process in a serial reactor configuration.  
25  
26 609 *Bioresour. Technol.* 264, 140–147.  
27  
28 610 <https://doi.org/10.1016/j.biortech.2018.05.070>  
29  
30  
31  
32 611 Tsapekos, P., Alvarado-Morales, M., Angelidaki, I., 2022. H<sub>2</sub> competition between  
33  
34 612 homoacetogenic bacteria and methanogenic archaea during biomethantion from  
35  
36 613 a combined experimental-modelling approach. *J. Environ. Chem. Eng.* 10,  
37  
38 614 107281. <https://doi.org/10.1016/j.jece.2022.107281>  
39  
40  
41  
42 615 Vermeij, P., Pennings, J.L., Maassen, S.M., Keltjens, J.T., Vogels, G.D., 1997. Cellular  
43  
44 616 levels of factor 390 and methanogenic enzymes during growth of  
45  
46 617 *Methanobacterium thermoautotrophicum* deltaH. *J. Bacteriol.* 179, 6640–6648.  
47  
48 618 <https://doi.org/10.1128/jb.179.21.6640-6648.1997>  
49  
50  
51 619 Wahid, R., Mulat, D.G., Gaby J.C., Horn, S.V., 2019. Effects of H<sub>2</sub>:CO<sub>2</sub> ratio and H<sub>2</sub>  
52  
53 620 supply fluctuation on methane content and microbial community composition  
54  
55  
56  
57  
58  
59  
60  
61  
62  
63  
64  
65

1 621 during *in-situ* biological biogas upgrading. *Biotechnol Biofuels* 12, 104.  
2  
3 622 <https://doi.org/10.1186/s13068-019-1443-6>  
4  
5 623 Wick, R.R., Judd, L.M., Gorrie, C.L., Holt, K.E., 2017. Unicycler: Resolving bacterial  
6  
7  
8 624 genome assemblies from short and long sequencing reads. *PLOS Comput. Biol.*  
9  
10 625 13, e1005595. <https://doi.org/10.1371/journal.pcbi.1005595>  
11  
12 626 Xu, J., Bu, F., Zhu, W., Luo, G., Xie, L., 2020. Microbial Consortia of  
13  
14  
15 627 Hydrogenotrophic Methanogenic Mixed Cultures in Lab-Scale Ex-Situ Biogas  
16  
17  
18 628 Upgrading Systems under Different Conditions of Temperature, pH and CO.  
19  
20 629 *Microorganisms* 8, 772. <https://doi.org/10.3390/microorganisms8050772>  
21  
22  
23 630  
24  
25 631  
26  
27  
28  
29  
30  
31  
32  
33  
34  
35  
36  
37  
38  
39  
40  
41  
42  
43  
44  
45  
46  
47  
48  
49  
50  
51  
52  
53  
54  
55  
56  
57  
58  
59  
60  
61  
62  
63  
64  
65

1 632 **Figure captions:**

2  
3 633 **Figure 1: Relative abundance of microbial taxa inferred from Illumina MiSeq**

4  
5  
6 634 **sequencing of 16S rRNA genes. (A)** Archaeal abundance at the genus level from the

7  
8 635 V4-V5 16S rRNA region of the 16S rRNA gene. The pie chart on right indicates

9  
10 636 abundance of minor genera (<2% of total archaeal reads). **(B)** Bacterial abundance at

11  
12 637 the phylum level from the V3-V4 16S rRNA region of the 16S rRNA gene. The pie

13  
14 638 charts on right show the proportion of the different classes and genera constituting the

15  
16  
17  
18 639 phyla *Bacillota* and *Pseudomonadota*.

19  
20 640 **Figure 2: Comparative genomics of strain Clermont. (A)** Phylogenomic tree of

21  
22 641 major archaeal clades based on a 73 genes core set using GToTree v1.8.2. **On left:**

23  
24 642 Known major clades, including *Methanothermobacter* (dark pink) are collapsed and

25  
26 643 shown as wedges of different colors. *Halobacteriales* was placed as outgroup. Bar, 0.3

27  
28 644 substitution per amino acid position. **On right:** Decollapsed *Methanothermobacter*

29  
30 645 wedge showing the position of strain Clermont (in red) within this genus. Bar, 0.05

31  
32 646 substitution per amino acid position. **(B)** Collinearity analysis among assemblies of the

33  
34 647 seven genomes forming the Marburg clade using MUMmer v4.0.0rc1 and visualized

35  
36 648 using NGenomeSyn. **(C)** Anvi'o representation of the pan-genome of the Marburg

37  
38 649 clade. Gene clusters (n = 2076) were ordered according to a hierarchical clustering of

39  
40 650 their presence/absence (inner dendrogram). Rings show the presence (filled) or absence

41  
42 651 (undashed) of the gene clusters in each genome. Single copy core and other core: gene

43  
44 652 clusters present in all seven *Methanothermobacter* genomes. Gene clusters exclusively

45  
46 653 present in a unique genome are indicated by a number: 1. strain K4, 2. strain THM\_2, 3.

47  
48 654 JZ-3\_D\_bin\_25, 4. strain Kepco-1, 5. GMQ\_75\_MeOH\_H2\_bin\_21, 6. strain Marburg,

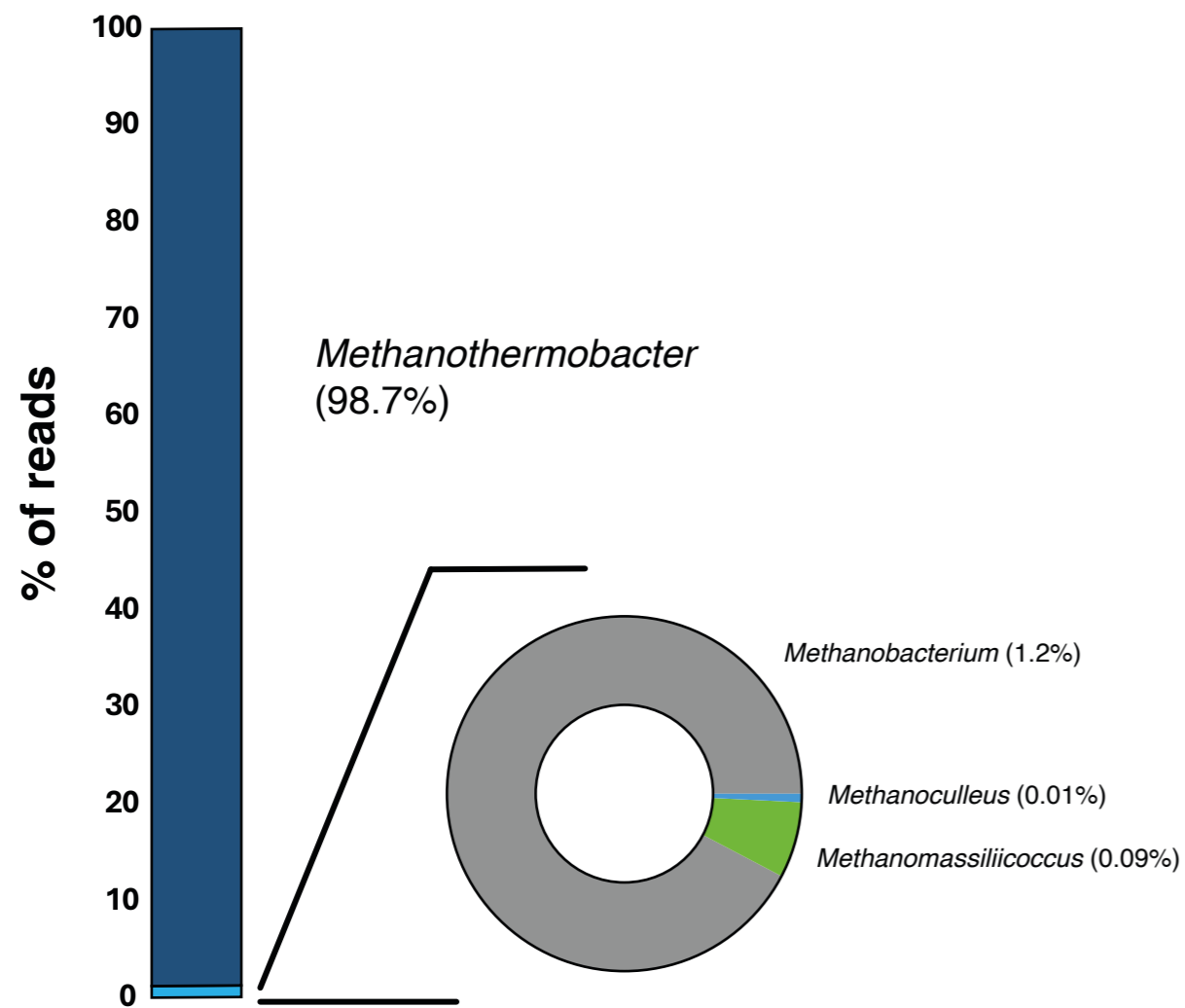
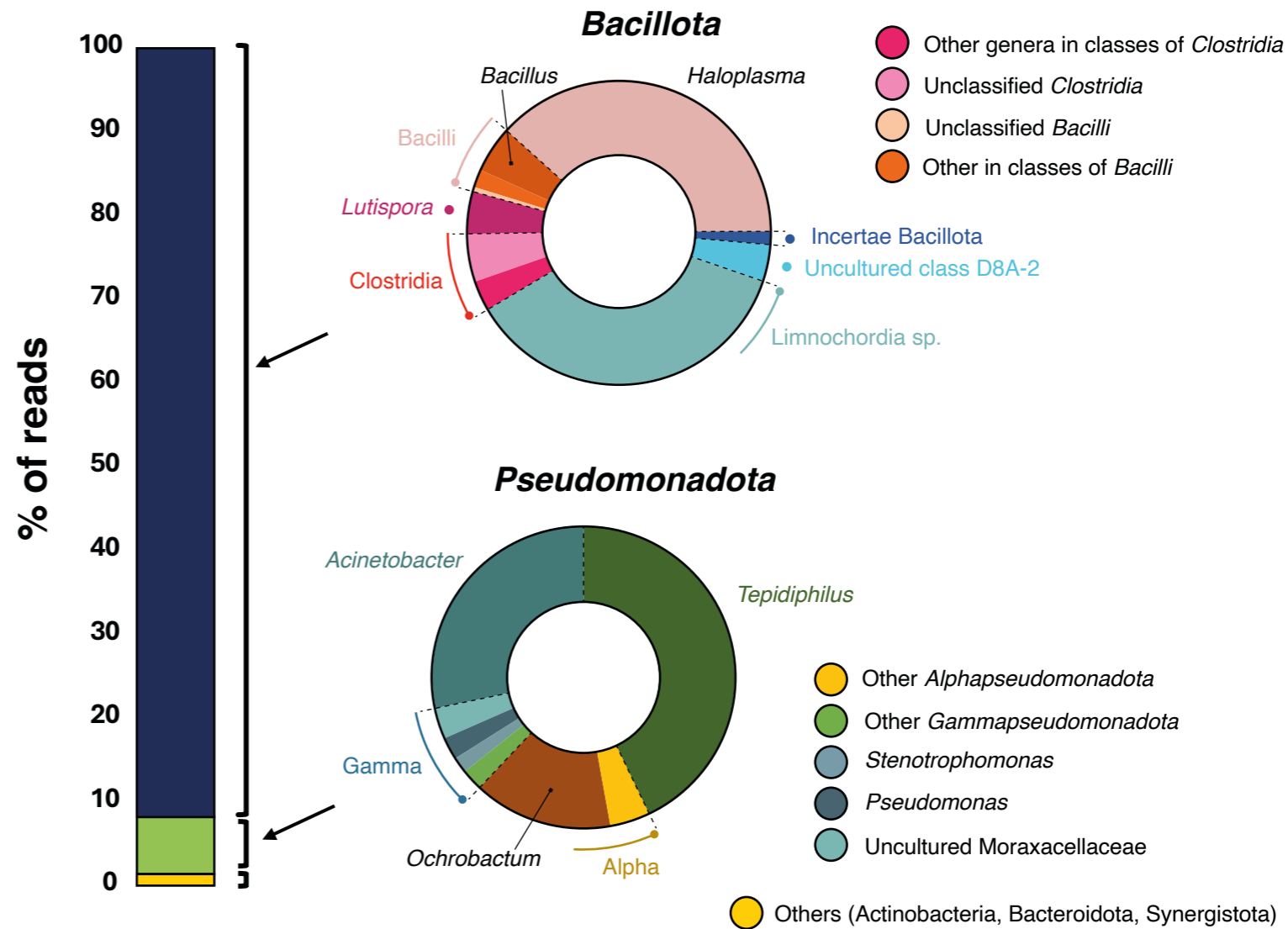
1 655 7. strain Clermont. To the right is given an ANI percentage identity heatmap; red: 100%  
2  
3 656 identity; light red: values ranging from 96% to 97%; white: values <96%.

4  
5  
6 657 **Figure 3: Methane yield under reduced conditions in batch culture for pure strains**  
7  
8 658 **(i.e. Marburg and Clermont) and the mixed adapted culture.** An asterisk denotes a  
9  
10 659 significant difference ( $p < 0.05$ ) between strain Marburg versus the two other cultures  
11  
12  
13 660 (days 3 to 6), and between the mixed culture versus pure cultures (days 8 and 18). The  
14  
15 661 error bar indicates the standard error (n=3).

16  
17  
18 662 **Figure 4: Methane yield in batch cultures under oxidative stressed conditions (240**  
19  
20 663 **min of exposure to O<sub>2</sub>).** (A) Comparison over time between strain Clermont and mixed  
21  
22 664 adapted culture. (B) Comparison over time between strain Clermont and strain Marburg.  
23  
24 665 An asterisk denotes a significant difference ( $p < 0.05$ ) between cultures over time. The  
25  
26 666 error bar indicates the standard error (n=3).

27  
28  
29  
30 667 **Figure 5: Schematic representation of oxidative stress protection enzymes detected**  
31  
32 668 **in the Marburg clade genomes.** (A) Gene-loci in the genome of strain Marburg. (B)  
33  
34 669 Potential cellular responses to oxidative stress.

35  
36  
37 670  
38 671  
39  
40  
41  
42  
43  
44  
45  
46  
47  
48  
49  
50  
51  
52  
53  
54  
55  
56  
57  
58  
59  
60  
61  
62  
63  
64  
65

**A****B**



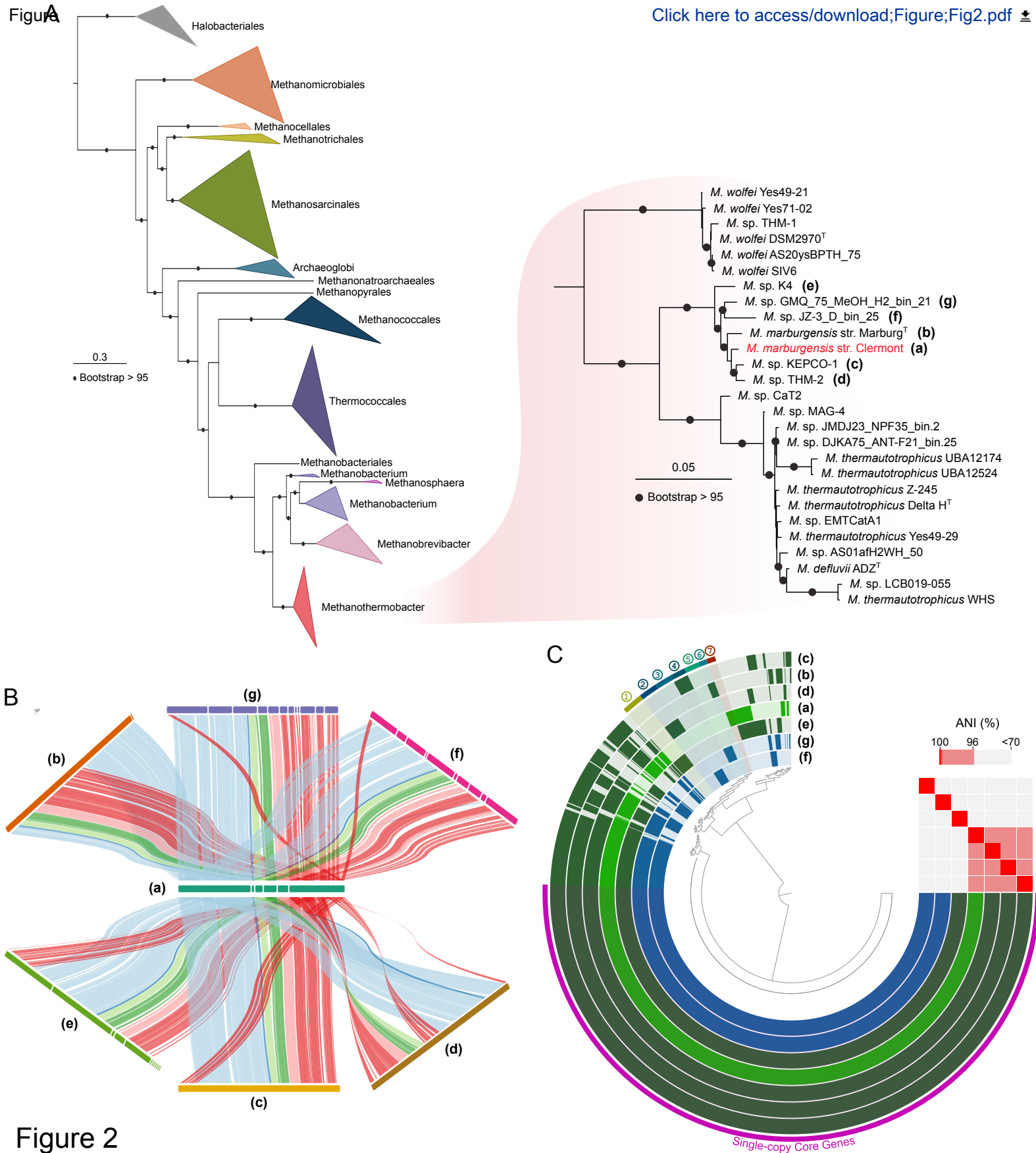


Figure 2

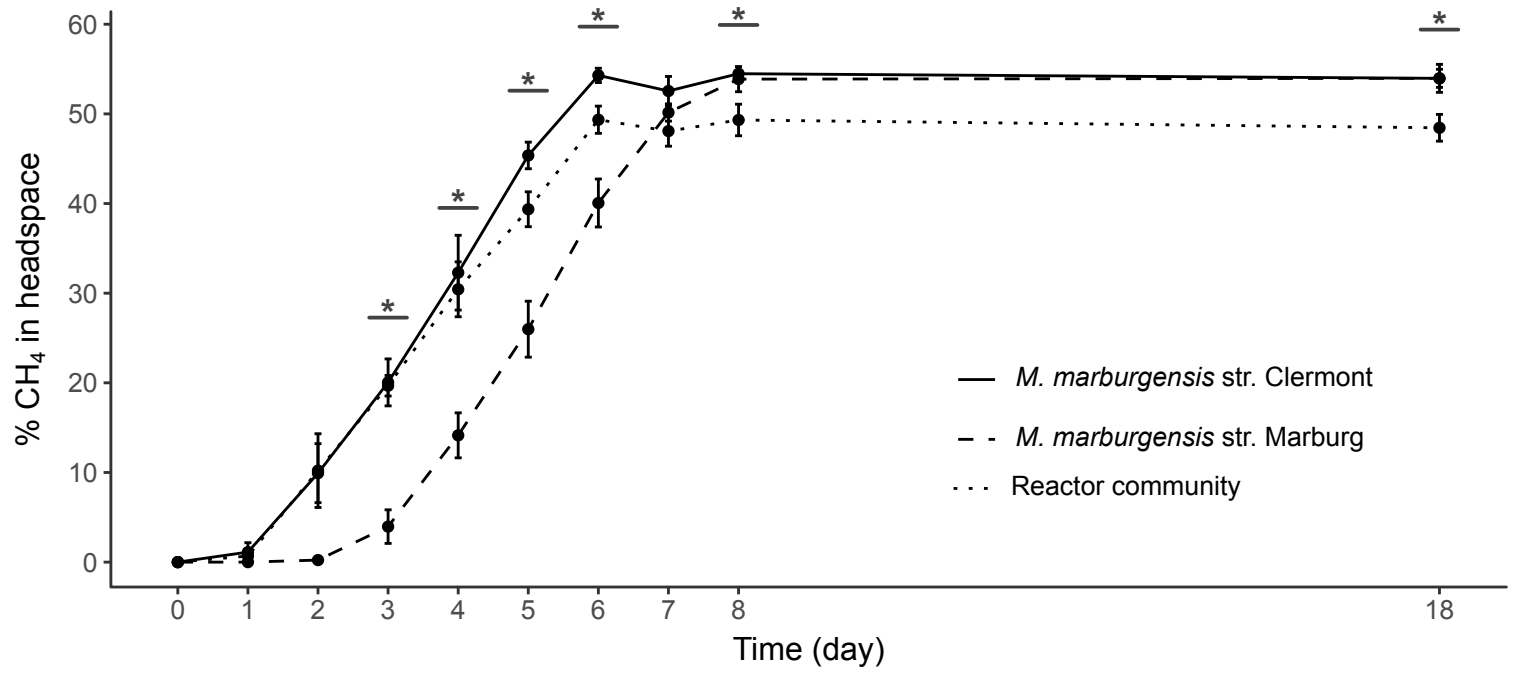


Figure 3

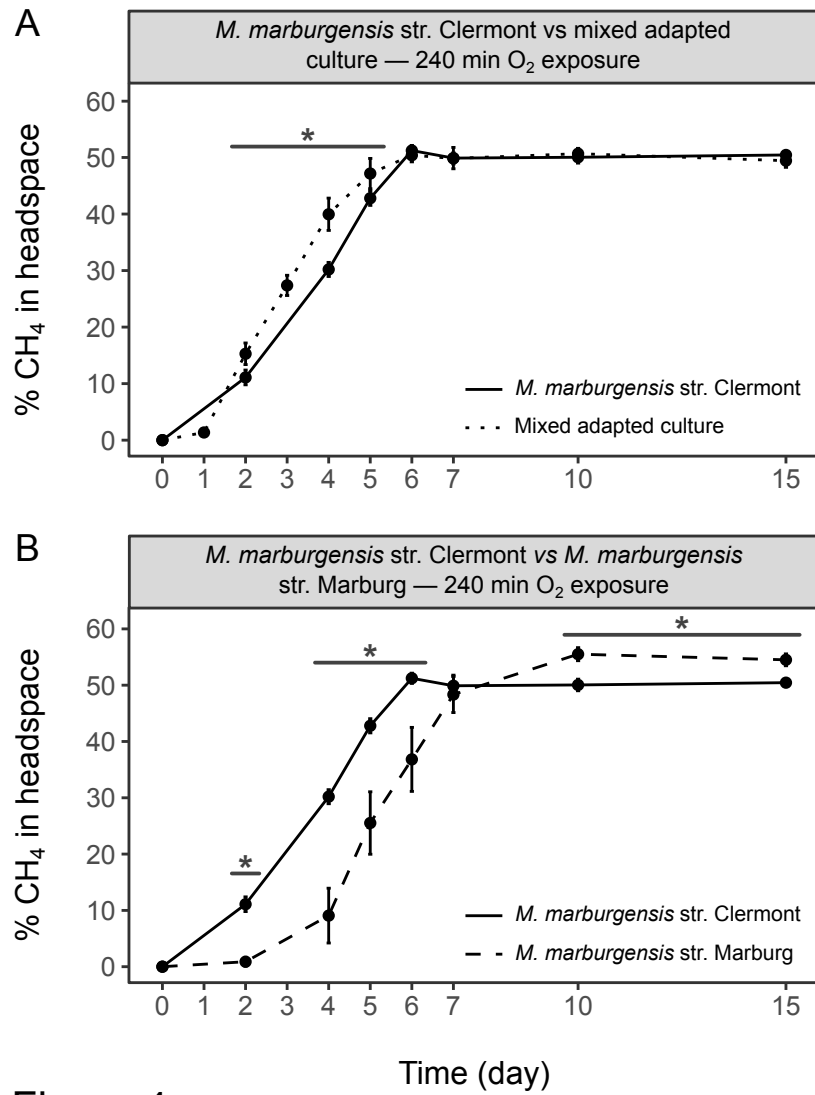
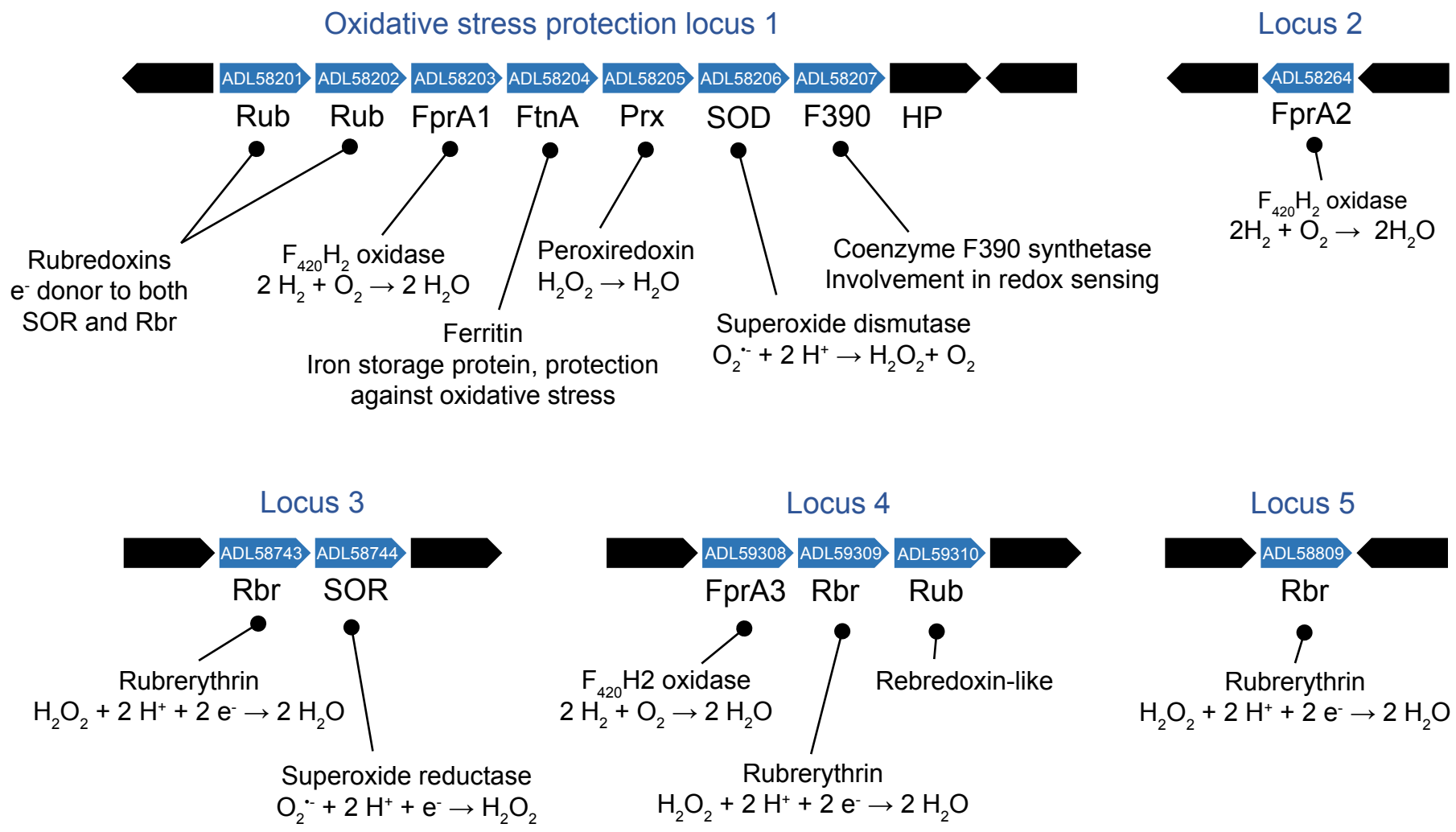


Figure A



B

O<sub>2</sub>/ROS elimination

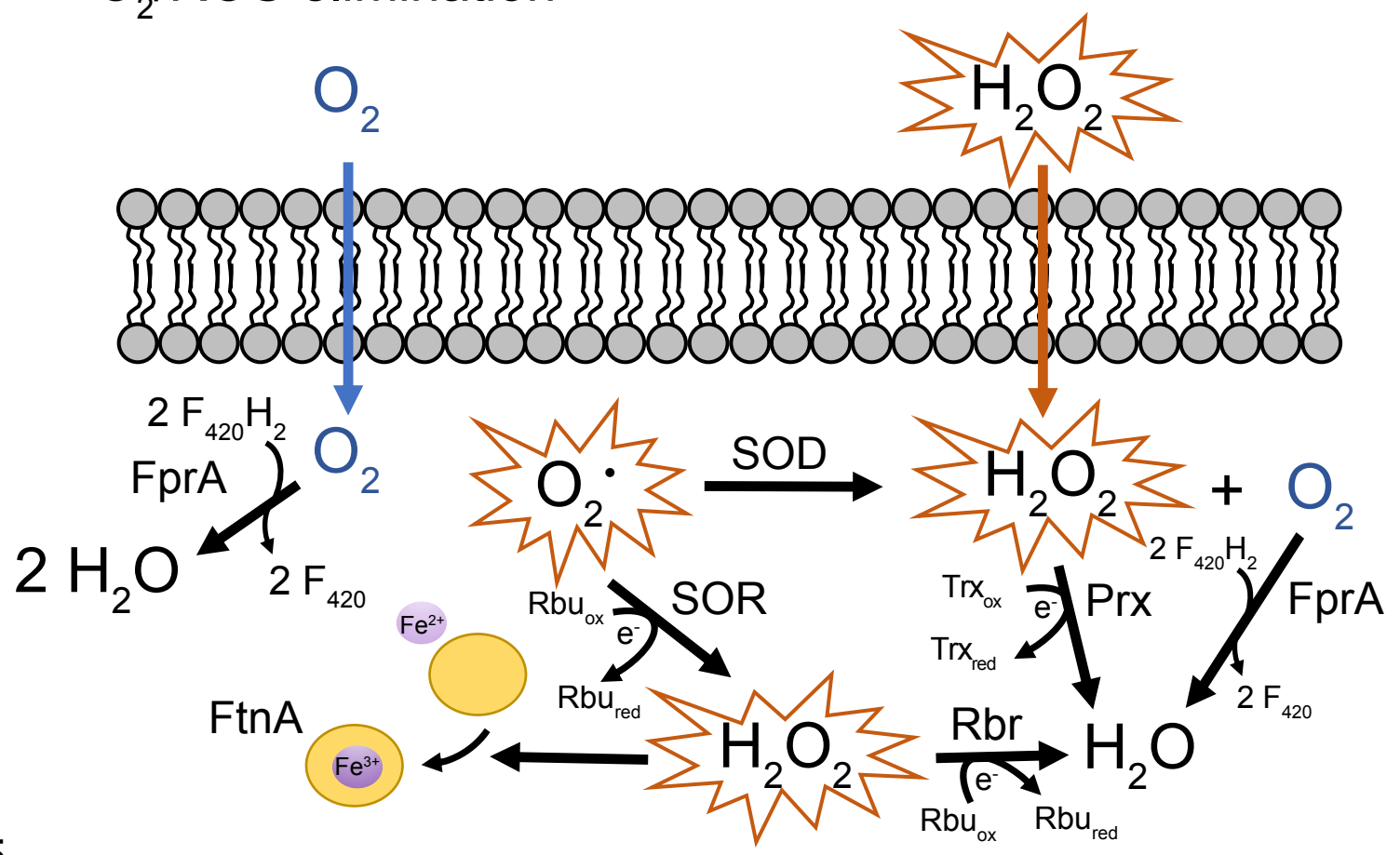


Figure 5

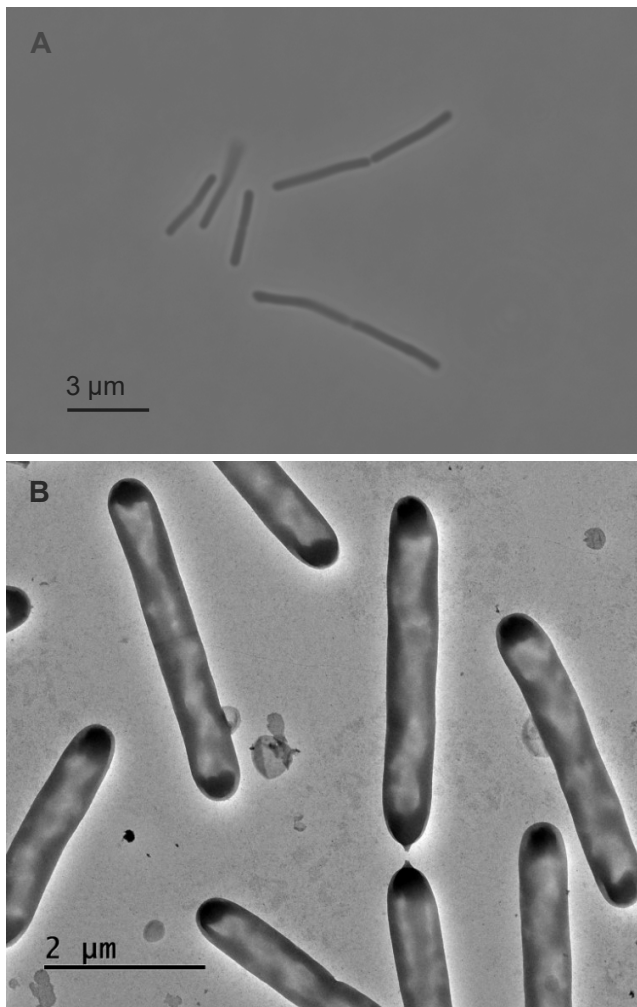


Figure S1: Morphology of *Methanothermobacter marburgensis* strain Clermont in optical microscopy (A) and transmission electron microscopy (B).

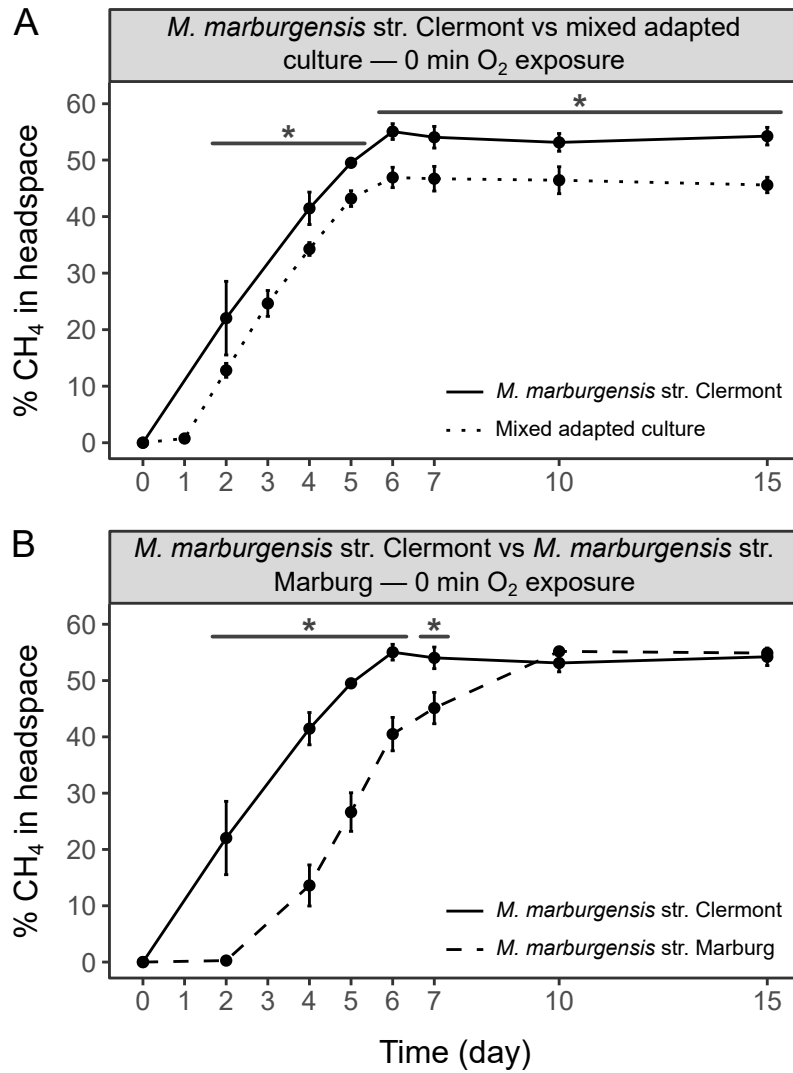
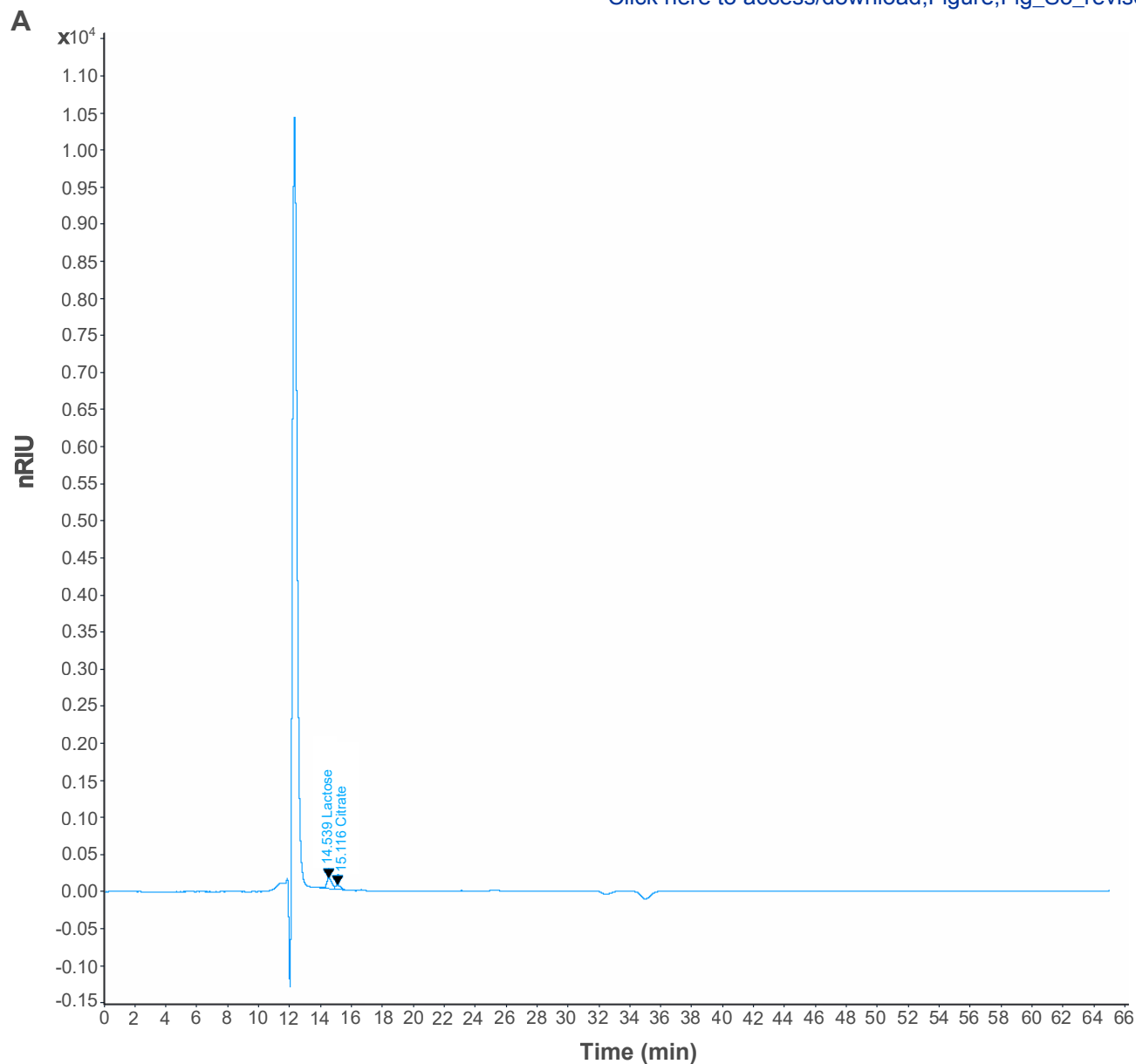


Figure S2: Methane production in batch cultures at the first level (0 min of exposure to  $\text{O}_2$ ) of the experiment oxidative stressed conditions. (A) Comparison over time between strain Clermont and the mixed adapted culture. (B) Comparison over time between strain Clermont and strain Marburg. Asterisks denote a significant difference ( $p < 0.05$ ) between cultures over time. The error bar indicates the standard error ( $n=3$ ).



**B**

Age	Citrate	Lactate	Acetate	Propionate	Butyrate	Succinate	Ethanol	Lactose	Glucose
0	0.017	0	0	0.054	0	0	0	0.033	0
43	0.015	0	0	0.017	0	0	0	0.032	0
46	0.015	0	0	0	0	0	0	0.036	0
50	0.016	0	0	0	0	0	0	0.036	0
54	0.014	0	0	0	0	0	0	0.032	0

Figure S3: Organic acids, ethanol, lactose, and glucose concentrations measured by liquid chromatography in mixed adapted cultures. (A) Chromatogram for the six-week mixed adapted culture used in the study (age 46 days post inoculation of bubble column reactor with digestate sample). (B) Concentrations for mixed adapted cultures of different ages (0 to 54 days post inoculation) including that used in the study (in blue, 46 days).





### Declaration of interests

The authors declare that they have no known competing financial interests or personal relationships that could have appeared to influence the work reported in this paper.

The authors declare the following financial interests/personal relationships which may be considered as potential competing interests:

Pierre Fontanille has patent #Procède de biométhanation in situ Number FR2211561 pending to neither licensee nor assignee. The authors declare that the strain *Methanothermobacter marburgensis* strain Clermont presented in this work was deposited according to the Budapest Treaty (rule 11.2, option 1) for the purposes of patent (filed on 7 november 2022). The authors declare that they have no known competing interests. If there are other authors, they declare that they have no known competing financial interests or personal relationships that could have appeared to influence the work reported in this paper.